UNIVERSITA' POLITECNICA DELLE MARCHE

SCUOLA DI DOTTORATO IN MEDICINA E CHIRURGIA

CURRICULUM "SALUTE DELL'UOMO"

Ph.D. Thesis

Trophoblast cell-surface antigen 2 and miR-125b: from normal human placental development to gestational diseases

Ph.D. candidate

Dr. Caterina Licini

Tutor

Prof. Daniela Marzioni

XXX cycle

Sommario

1. Introduction

1.1. Placenta

Placenta is a foetal origin organ and it is fundamental in pregnancy (Figure 1). Its main role is to manage metabolic and catabolic exchanges (gases, nutrients and waste products) between foetus and mother during gestation. Other functions are the synthesis and secretion of hormones, that regulate placental, foetal and maternal systems, and the immunological regulation, in order to prevent rejection of the foetal allograft. (1)

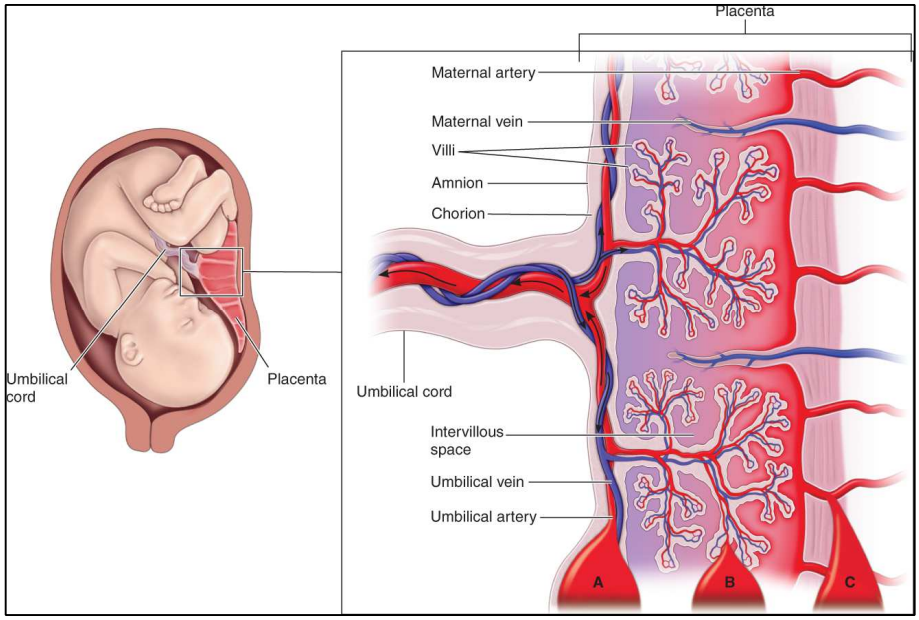

Figure 1- Foetus and the placenta anatomy. (2)

1.1.1. Early development of the human placenta

The development of placenta starts with the invasion of the uterine wall by the blastocyst. During attachment and after invasion of the endometrial epithelium, the outer layer of the embryonic pole of the blastocyst is transformed to syncytiotrophoblast by fusion of the neighbouring trophoblast cells. The residual

cells remain temporally unfused and are called cytotrophoblast cells. During the prelacunar stage (Figure 2a, 2b), between the 6th and the 8th day postcoitus (p.c.), the syncytiotrophoblast invades and corrodes the maternal endometrium, starting the placenta development. In this way, these cells continue the placenta formation close contact to the uterine mucosa.

During the lacunar stage (until the 13th day p.c.), trophoblast (syncytio- and cytotrophoblast) continues to proliferate and invade the endometrium, forming vacuoles called lacunae, rounded by syncytiotrophoblast lamellae, the trabeculae (Figure 2c, 2d).

Lacunar formation subdivides the trophoblast of the blastocyst in three layers: the primary chorionic plate, which is composed mainly of cytotrophoblast; the lacunar system with the trabeculae; the trophoblastic shell, facing the endometrium. Around the 12th day, the cytotrophoblast from the primary chorionic plate begins to invade the trabeculae for the whole length, forming the primary villi, that increase in length and diameter (Figure 2d). The lacunar system become the intervillous space.

The endometrial stroma during this process is subjected to the erosion by the trophoblast. These hormonal and mechanical input stimulates the endometrial stromal cells to proliferate and to enlarge, giving rise to the decidual cells. The invasive activity of the trophoblast causes the disintegration of the endometrial vessel walls from the 12th day; in this way, the maternal blood enters in the lacunae in order to start the foetal-maternal circulation (Figure 2d).

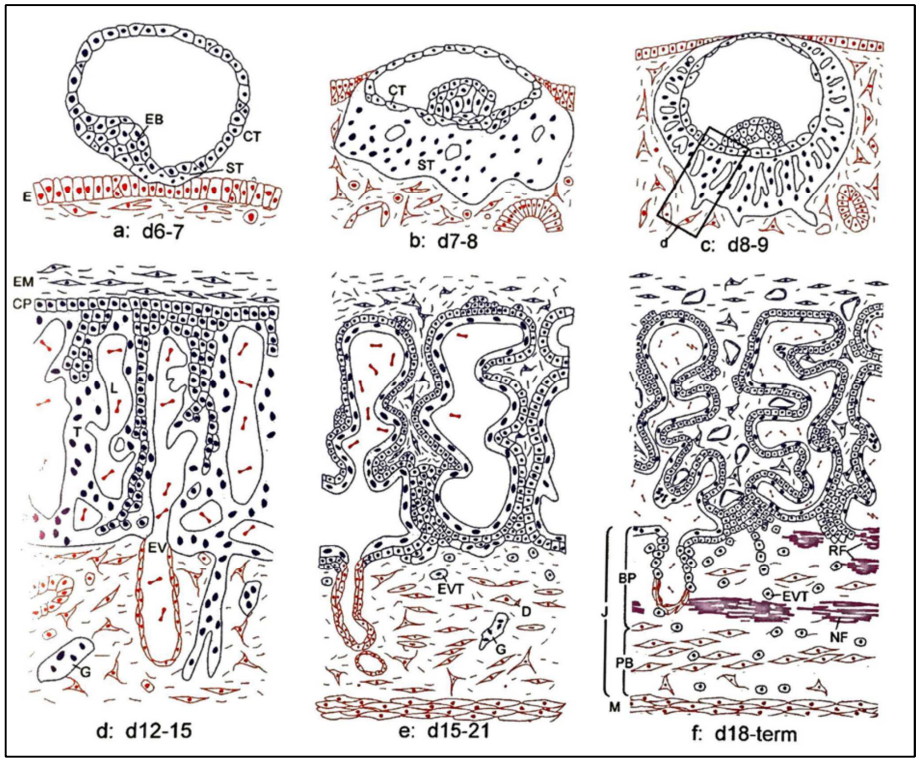

Figure 2- Development of the placenta. Prelacunar stage (a, b); lacunar stage (c); transition from lacunar stage to primary villous stage (d); secondary villous stage (e); tertiary villous stage (f). (3)

Between the 15th and the 21th day p.c., mesenchymal cells derived from the extraembryonic mesenchyme layer of the primary chorionic plate begin to invade the villi, transforming them in secondary villi (Figure 2e). The basal segments of the trabeculae are formed by clusters of cytotrophoblast surrounded by a thin and incomplete sheet of syncytiotrophoblast. These structures, called cell columns, are places of longitudinal growth of anchoring villi, as well as sources of extravillous trophoblast.

Between the 18th and the 20th day p.c., the first foetal capillaries can be observed in the mesenchyme. The appearance of cross section of capillaries in the villous stroma marks the development of the first tertiary villi (Figure 2f). A complete

foetomaternal circulation is established at the beginning of the 5th week p.c., until the delivery.

Foetal and maternal bloods come very close as soon as an intravillous circulation is established. However, the two bloodstreams are always separated by the placental barrier. (3)

1.1.2. Basic structure of the villous tree

The main part of the placenta in the foetomaternal circulation is the villous tree. It consists of a structure that origins from the chorionic plate and protrude into the intervillous space, where the maternal blood is present. The villous tree is formed by a central "trunk" with numerous specialized branches, called chorionic villi. During the placenta development, different types of villi show different structural and functional specialization. Despite these modifications, all the villi have the same basic structure: syncytiotrophoblast, cytotrophoblast, trophoblastic basement membrane, stroma, foetal vessels (Figure 3a, 3b).

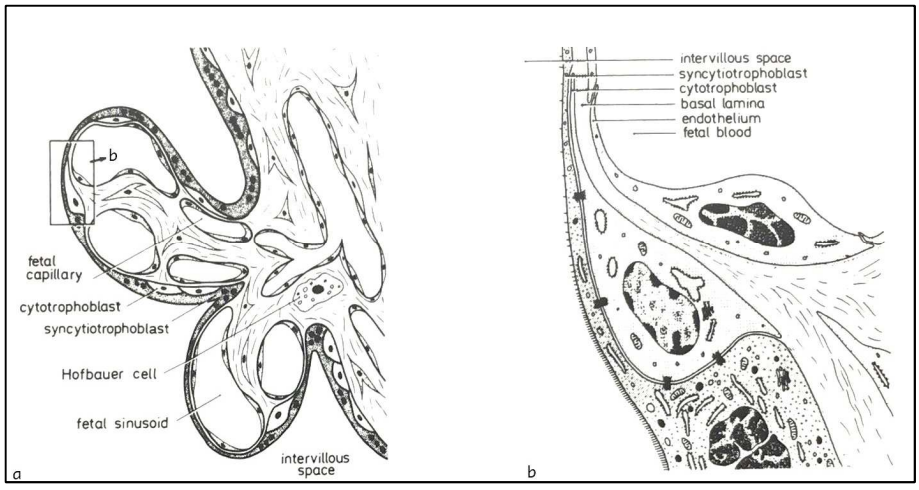

Figure 3- Section of the placental villus (a); particular (b). (3)

Villi are covered by syncytiotrophoblast, an epithelial surface layer that separates the villous core and the maternal blood which flows in the intervillous space. Syncytiotrophoblast is composed by a continuous multinucleated cell layer. Syncytial knots are a syncytiotrophoblastic features composed by aggregated nuclei that bulge slightly on the trophoblastic surface. Their number increases in many pathological conditions, such as preeclampsia and preeclampsia complicated by IUGR.

Under the syncytiotrophoblast layer, there is the cytotrophoblast, a layer of single or aggregated cells, which acts as the "stem cells" of the syncytiotrophoblast.

At the structural signs of syncytial degeneration, cytotrophoblast cells proliferate by mitosis and, while one of the daughter cells conserves its stem property, the other one starts apoptosis that stimulates the syncytial fusion (Figure 4). In this way, the cytotrophoblast cell becomes part of the upper syncytiotrophoblast. As soon as the syncytial degeneration starts again, this process begins again. In this way, a large number of nuclei accumulate in the syncytiotrophoblast, and some of them are clustered as syncytial knots (Figure 4).

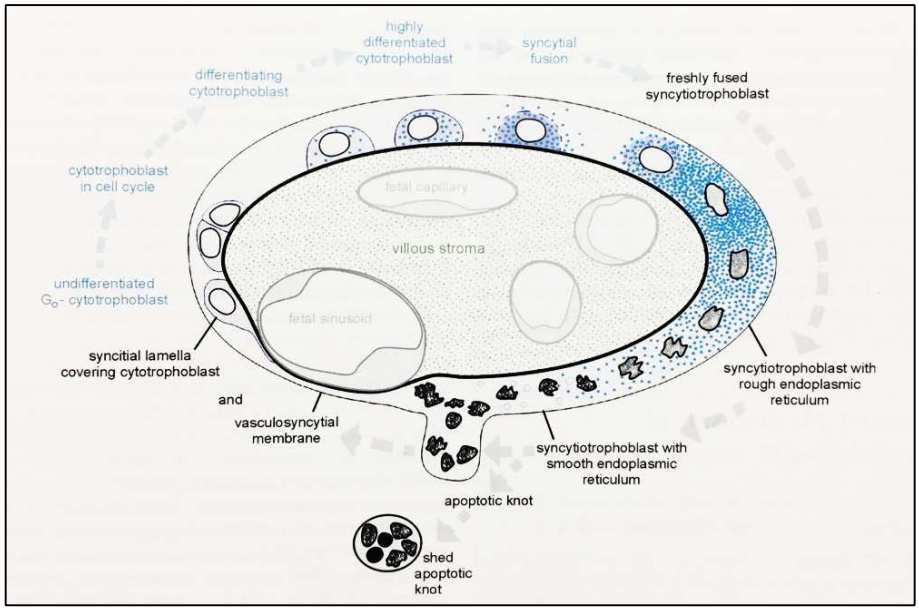

Figure 4- Schematic representation of trophoblast turnover and trophoblastic apoptosis al the villous surface (3)

The trophoblastic basement membrane separates syncytiotrophoblast and cytotrophoblast from the stroma of the villi.

The stroma is the internal part of villi and it is composed by fixed connective cells that form a network with connective tissue fibres, free connective tissue cells (i.e. macrophages called Hofbauer cells) and foetal vessels. The stroma composition depends on the age of the placenta, on the type of villous, and on the position of the villous. The stroma can include mesenchymal cells, fibroblasts, myofibroblasts, extracellular matrix protein (collagen I, III, IV, and VI; fibronectin isoforms), reticular fibres, proteoglycans and matrix-degrading proteolytic enzymes (that are involved in remodelling during the placental development).

In the villous stroma, there are foetal vessels of various kinds and calibres. In the stem villi, the vessels are mainly arteries and veins. In the smaller villi, there are mainly capillaries and sinusoids.

Five types of villi have been described. Mesenchymal villi are the most primitive and prevail during the first stages of pregnancy. They are the forerunners of immature intermediate villi. Histologically, they have a thick trophoblastic surface with large number of cytotrophoblast cells between the syncytiotrophoblast and the basal lamina. The stroma contains loosely arranged collagen fibres and foetal capillaries poorly developed. (Figure 5)

Stem villi are a group of different part of the villous tree that shows similar histological features but differs from each other in calibre and position in the villous branching.

They are characterised by a condensed fibrous stroma with arteries and veins or arterioles and venules. The trophoblastic cover is uniformly thick and cytotrophoblastic cells can be found on about the 20% of the villous surface. (Figure 5) In mature placenta, the trophoblast is often degenerated and replaced by fibrinoids.

Immature intermediated villi are peripheral, immature continuations of stem villi and they prevail in immature placenta. Histologically, they have a thick trophoblastic cover and cytotrophoblast cells can be found on the 50% of the villous surface. They have a reticular stroma, with numerous channels that contain Hofbauer cells suspended in some fluid. Foetal vessels are placed between these channels. (Figure 5)

Mature intermediate villi are characterized by stroma with loose bundles of connective tissue and fixed connective tissue cells and contain numerous capillaries, small arterioles and venules. (Figure 5)

Terminal villi originate from mature intermediate villi and they appear in the last trimester of pregnancy. They are characterised by a thin trophoblastic cover and sinusoidal capillaries that occupy more than 50% of the villous stroma. (Figure 5) The sinusoids are close contact to trophoblastic surface and it is important for diffusional exchanges because of the small distance for the foetomaternal diffusion. (3)

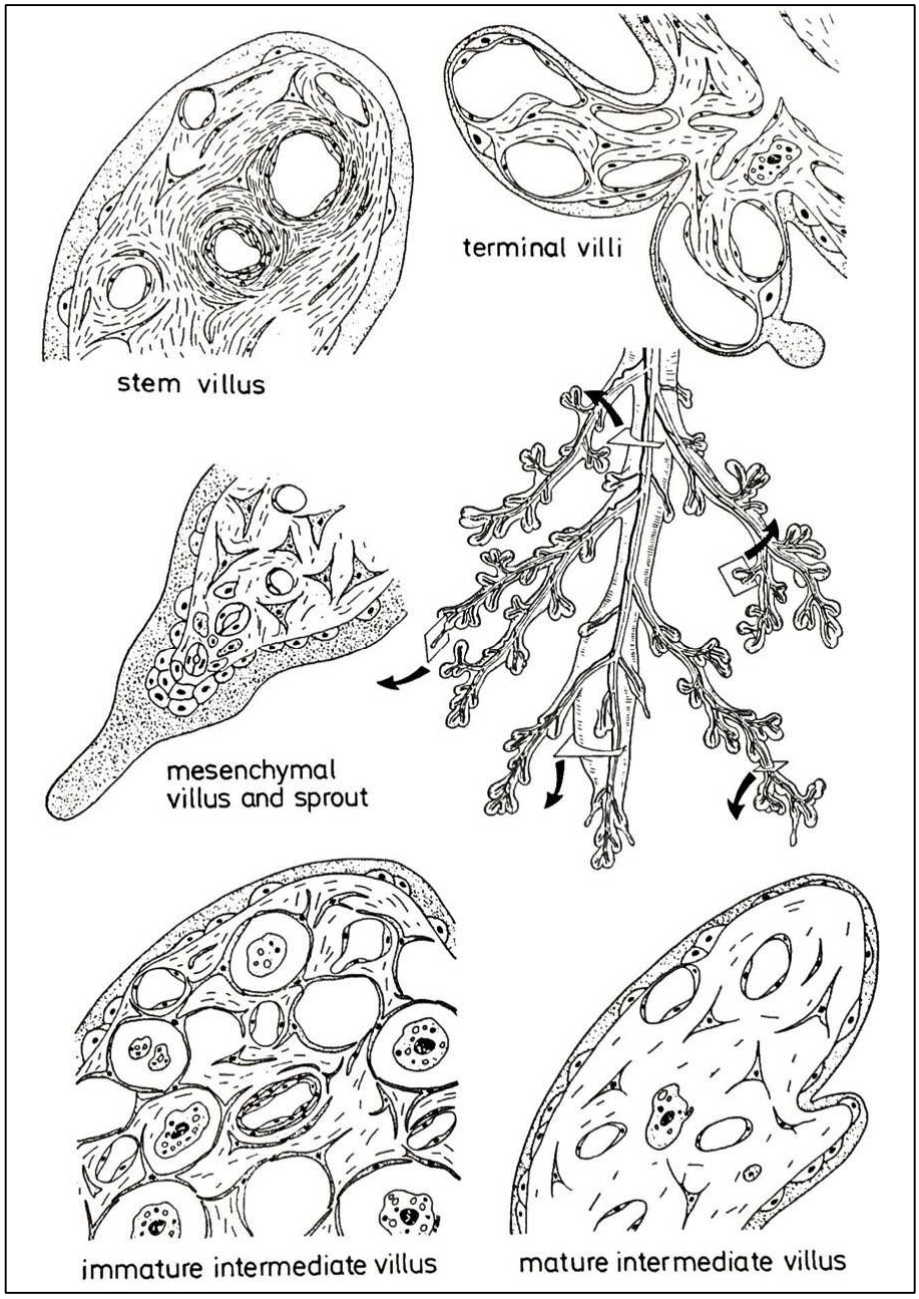

Figure 5- Representation of a mature villous tree and cross sections of types of chorionic villi. (3)

1.1.3. Nonvillous parts of the placenta

The main nonvillous parts of the placenta are the chorionic plate, basal plate, cell islands, cell columns, placental septa. They don't participate in foeto-maternal exchanges since they are not vascularized by both circulations (maternal and foetal). The basic components of these structures are extravillous trophoblast and

fibrinoids mainly. The extravillous trophoblast is an epithelially derived tissue and it originates from the trophoblastic wall of the blastocyst. For definition, extravillous trophoblast represents the trophoblast cells that have migrated out of the villous trees and can be found in all the parts of placenta (Figure 6).

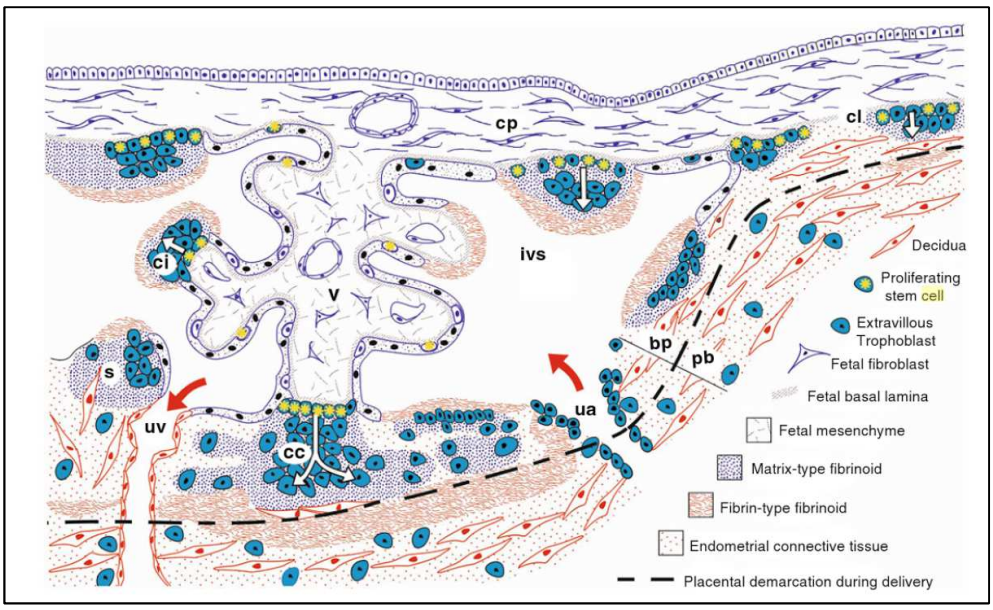

Figure 6- Representative drawing of the various part and cell population of the human placenta; amnion (a); chorionic plate (cp); chorion leave (cl); intervillous space (ivs); septa (s); uteroplacental arteries (ua); uteroplacental veins (uv); cell column (cc); cell island (ci); septa (s); basal plate (bp); placental bed (pb). (3)

Extravillous trophoblast cells originate at the tips of the anchoring villi, where they form the cell columns. The cell columns connect the anchoring villi to the placental septa that subdivide incompletely the intervillous space. Accumulation of extravillous trophoblast cells can be found in correspondence of several villi, in continuous with cytotrophoblast where syncytiotrophoblast is interrupted. These accumulations are called cell islands.

The chorionic plate is the part of the placenta in contact with the amnion, the membrane that contains the embryo first and the foetus then. It is vascularized by the foetal vessels only. On the outer part of the chorionic plate there is the insertion of the umbilical cord. The villous tree arises from the internal part of the chorionic plate and protrude into the intervillous space.

At the opposite part of the placenta, there is the basal plate, that is the portion of the placenta in contact with the uterus and it is vascularized by the maternal vessels only. It is constituted by embryonic tissue (extravillous trophoblast) and maternal tissue (decidua). (3)

1.2. Preeclampsia and IntraUterine Growth Restriction

Hypertensive diseases occur in approximately 12-22% of pregnancies and, often, there is confusion about the different disorders. The American Congress Obstetrician and Gynecologists (ACOG) defines hypertension as a systolic blood pressure level of ≥ 140 mmHg and/or diastolic blood pressure level of ≥ 90 mmHg that occurs after 20 weeks of gestation in a woman with normal blood pressure previously. About one in four hypertensive women develops proteinuria, and hypertension evolves in preeclampsia. Proteinuria is defined as the presence of 0,3 g or more of protein in a 24-hour urine specimen. (4,6).

Preeclampsia (PE) is a pregnancy-specific syndrome that involves approximately 5-8 % of pregnant women and is one of the leading causes of maternal and foetal mortality and morbidity. It is a heterogeneous disease and different classifications are based on severity (severe PE is defined as BP≥ 160 mm Hg systolic, DBP ≥ 105 mm Hg diastolic, or both) and onset of the clinical symptoms (early-onset PE

occurs before the 34th week of gestation and late-onset PE occurs after the 34th week of gestation) (5,7-9)

Women with mild forms of preeclampsia generally have uneventful deliveries and, after the deliveries, the disease ceases. Women with more severe forms can develop features, such as renal involvement, neurological sequelae, eclampsia, and HELLP syndrome (haemolysis, elevated liver enzymes, and low platelet count). In extreme cases, maternal death can occur, preceded by acute renal failure, hepatic rupture, pulmonary oedema, placental abruption, seizure, and coma. (3,10)

The main risk factor for preeclampsia are extremes of maternal age, multifetal gestation, preeclampsia in a previous pregnancy, chronic hypertension or renal disease, but also pregnancy after donor insemination, oocyte donation, obesity and insulin resistance, pregestational diabetes mellitus, maternal infections, family history of preeclampsia and smoking.(4,11)

The causes of preeclampsia remain not clear, but it is known that preeclampsia begins with the presence of the placenta or the maternal response to placentation. (11)

Systemic maternal vascular dysfunction is the major phenotype of pregnancies with preeclampsia, and changes in the oxygenation levels of the placenta due to failure of spiral artery transformation are thought to be responsible for increased peripheral vascular resistance, maternal hypertension and proteinuria. (6,12).

In addition to inadequate endovascular invasion, other dysfunctions, such as deficient trophoblast survival, endothelial cell dysfunction and a systemic

maternal inflammatory response, are involved in the aetiology of this condition. (13)

According to the "two-stage theory" of PE etiopathogenesis, an abnormal spiral artery remodelling in early pregnancy causes placental hypoxia (stage 1) and the ischemic placenta releases large amounts of soluble factors, such as reactive oxygen species, pro-inflammatory cytokines, and anti-angiogenic factors into the maternal circulation, which conduct to the clinical manifestations and complications of the disease (stage 2) (Figure 7). (7)

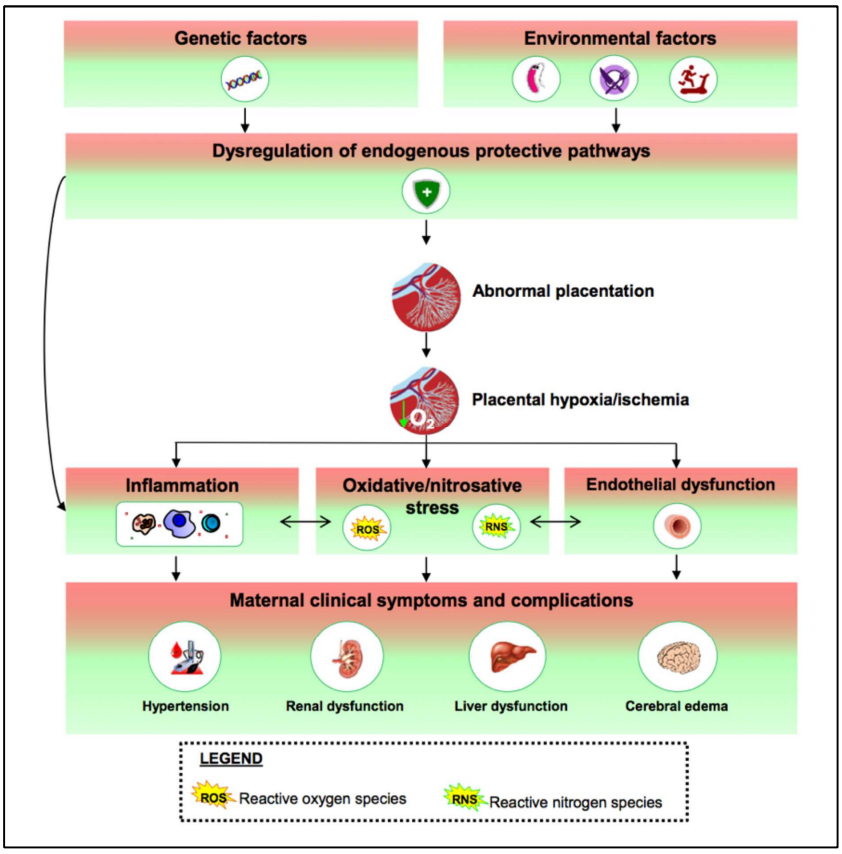

Figure 7- The "two stages" theory of PE etiopathogenesis (7)

Placenta in PE typically has normal weight and size, but it shows marked proliferation of villous cytotrophoblast cells and necrosis in syncytiotrophoblast cells. These proliferative disorders and the increased formation of syncytial knots are usually associated to PE disorder (Figure 8). (14,15)

The principal pathologic changes of placenta include decidual arteriolopathy, infarcts and ischemic change in the central portions of the placenta and abruptio placentae (3). Preeclampsia symptoms can be treated in different ways with different laboratory tests and therapies, depending on the severity of the disease. One of the possible treatment involves the use of the antihypertensive drugs. In case of women with increased risk of preeclampsia, strategies of prevention can be used. Magnesium sulphate can be used as prevention and treatment in women with severe preeclampsia.(4,10)

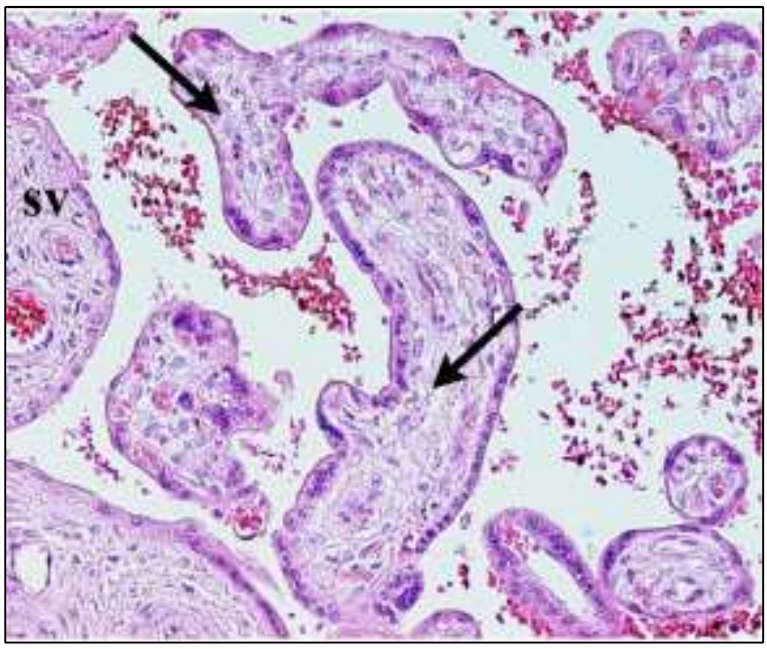

Figure 8- Haematoxylin and eosin staining of placenta with preeclampsia (14)

Intra-uterine growth restriction (IUGR) is sometimes associated with preeclampsia and, unlike PE, it is of foetal origin. IUGR is defined as a birth weight below the 10^{th} percentile for the gestational age and is the failure of the foetus to achieve his potential growth. (16,17)

IUGR disease predisposes the foetus and neonate to risk of death or disability in the perinatal period and the child to a lifelong increased risk for hypertension, cardiovascular disorders, renal disease, and other disorders. (18)

In case of pregnancy with IUGR, the placenta development is characterised by imbalances of injury and repair and maldevelopment of the villous tree. Villous cytotrophoblast exhibit enhanced sensitivity to undergo cell death in response to hypoxia and cytokines, when compared to control pregnancies. Excess injury of the villous trophoblast layer reduces the functional mass of syncytiotrophoblast in IUGR and limit the capacity of villi to mediate the nutrient transport. As syncytial knots reflect a characteristic feature of syncytiotrophoblast apoptosis, one sign of an overall increase in apoptosis in placentas from pregnancies with IUGR is the prominence of syncytial knots compared to the normal villous histology of control pregnancies (Figure 9). (18,19)

All these injuries produce some effects in placenta: small size, persisting immaturity, high degrees of infarction, foetoplacental vasculopathy, villous hyper maturity, terminal villous deficiency (3,20-21).

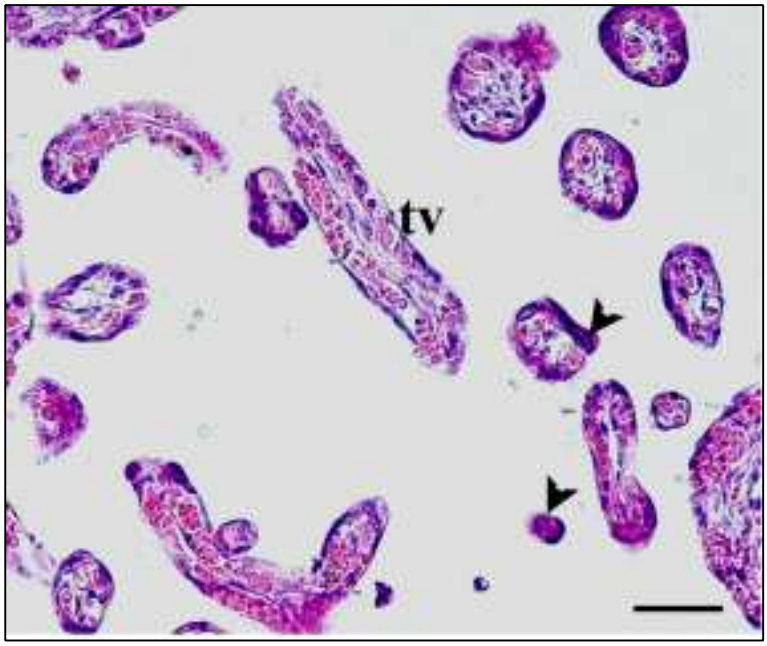

Figure 9- Haematoxylin and eosin staining of placenta affected by preeclampsia complicated by IUGR (14)

1.3. Trop-2

Human trophoblastic cell surface antigen 2 (*Trop-2*) gene, also known as tumour-associated calcium signal transducer (*tacstd2*), encode a 35-49 kDa transmembrane glycoprotein. (22)

Trop-2 protein was first identified by Lipinski as a marker for trophoblast cells and choriocarcinoma cell lines. (23)

It is composed by a large extracellular domain, a transmembrane domain and a short intracytoplasmic C-terminal tail (Figure 10). The cytoplasmic tail is required for cell growth and its absence hold the stimulation for cellular growth, and it contains a HIKE-like phosphoinositide-binding motif, that usually is involved in signalling transduction.

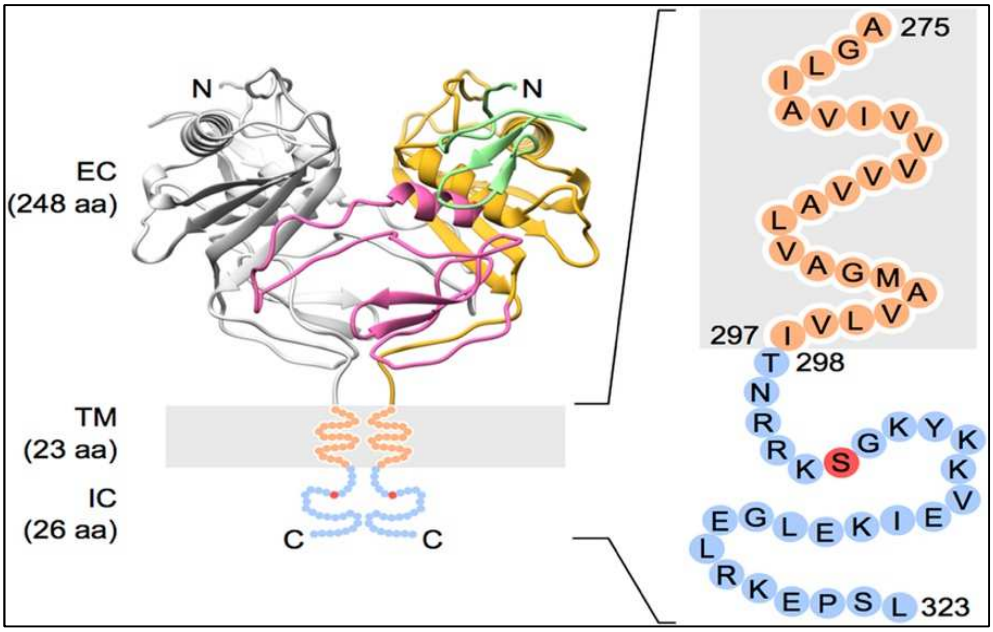

Figure 7- Trop-2 protein structure and cytoplasmic tail. The transmembrane (TM) and the intracellular tail (IC) are shown in orange and blue, respectively, and the conserved phosphorylation site (Ser303) within the IC is shown in red. (24)

1.3.1. Trop-2 mechanisms of action and role in cancer development

Trop-2 works as a cell surface receptor through the extracellular and transmembrane domain that transmit extracellular signals to the short cytosolic tail. (22,24-26)

Studies report that a Trop-2 biological function is the involvement in the regulation of tight junction formation, and therefore in cell-cell adhesion, binding and transporting claudin-1 and -7 to cell membrane, protecting them from degradation by the ubiquitin- proteasome system. (22,27)

However, the most studied Trop-2 function is its role in cell proliferation. (25,28-30)

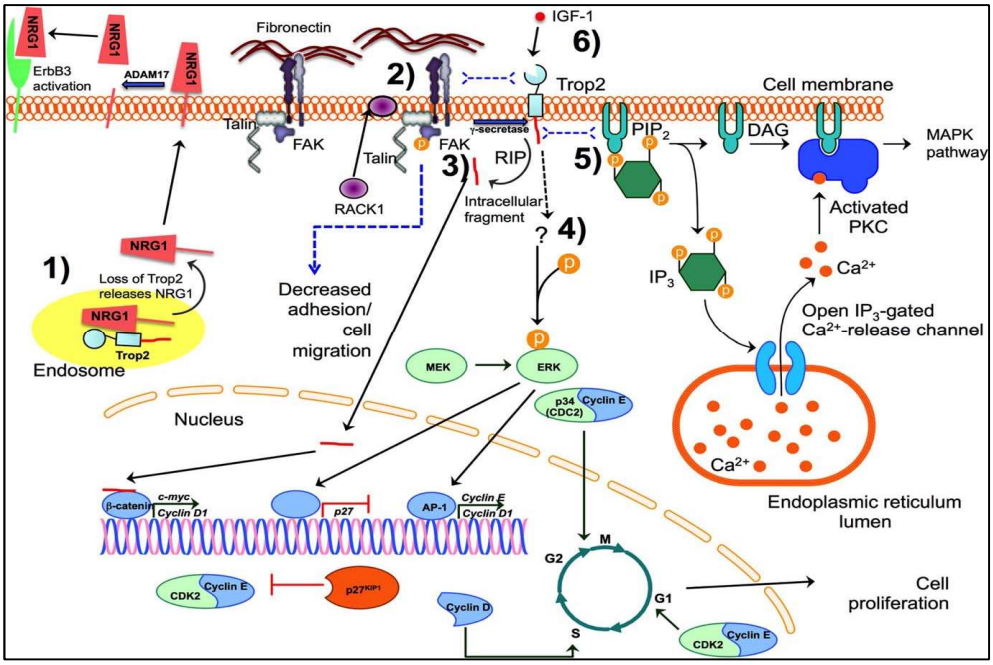

Figure 8- The principal pathways mediated by Trop-2 (22)

Trop-2 activation increases intracellular calcium concentrations. (31) The intracellular tail of Trop2 contains a putative PIP2 binding site, which is the likely pathway leading to increased calcium. Hydrolysis of PIP2 results in the production of DAG and IP3, that binds to the IP3 receptor (IP3R), resulting in release of calcium from endoplasmic reticulum (Figure 11).

Furthermore, Trop-2 undergoes regulated intramembrane proteolysis (RIP) at two cleavage sites mediated by the g-secretase complex and results in a large extracellular fragment and a short intracellular fragment. The intracellular fragment can enter the nucleus, where it binds to the b-catenin transcription factor, increasing the expression of cyclin D1 and c-myc (32), promoting cell proliferation and self-renewal. Another important pathway regulated by Trop-2 is the phosphorylation of ERK (Figure 11). (25,30,33) The ERK-mediated activity operates on AP-1 transcription factor, increasing the expression of cyclin D1,

cyclin E, and cyclin-dependent kinases (CDK), promoting cell cycle progression and cell proliferation. TROP2-mediated ERK activity also decreases cell cycle inhibitor p27/kip1, which inhibits the activity of the cyclin E/ CDK2 complex (Figure 11). (30) Through these pathways, Trop-2 acts on cell proliferation and cell motility and metastasis, affirming its important and fundamental role in the rise and the development of numerous types of cancer.

In fact, Trop-2 expression increases in numerous cancer types and, in several studies, is considered as one of the major tumorigenic factors for glioma, ovary, stomach, pancreas, colon and rectum, uterus and bladder cancer. (22,26,34-39) Guerra et al. showed that increased levels of Trop-2 expression is due to the overexpression of transcription factors in cancer cells and not to mutations or amplifications of *Trop-2* gene, confirming its functional role. (25)

In vitro analyses show as the ectopic expression of Trop-2 in a variety of cancer cell lines in culture increases cell proliferation and causes the cells to become highly tumorigenic when injected into mice. (30,40-42) Similarly, knock-down of Trop-2 using siRNA in colon cancer cells and in mammary tumour cells inhibited cell proliferation and the ability of the cells to form colonies in vitro. (40-41)

In addition to being critical for tumour growth, Trop-2 is also involved in metastasis. High Trop-2 expression has been correlated to increased metastasis in patients with colorectal cancer (37), pancreatic cancer (43), ovarian cancer (36), breast cancer (33), laryngeal squamous cell carcinoma (44), and extra nodal NK/T cell lymphoma, nasal type (45). Furthermore, Trop-2 is present in all distant metastases in humans with prostate cancer (42). In vitro, overexpression of Trop-2 increases the migration of pancreatic cancer cells (30), whereas inhibition of

Trop-2 using anti-Trop-2 antibodies decreases the migration of colon and breast cancer cells (40,46).

No studies on Trop-2 physiological and pathological placenta are present in literature.

1.4. MicroRNA e miR-125b

1.4.1. MicroRNA biogenesis

MicroRNAs (miRNAs) are small noncoding RNA (17-25 nucleotides) first described in *C. Elegans.* (47)

miRNA genes are transcribed by RNA polymerase II (Poll) to form primary miRNA (pri-mRNA), the primitive configuration characterized by a specially modified nucleotide at the 5′-end and a polyadenilated at the 3′-end. The Microprocessor Complex, formed by a nuclear protein known as DiGeorge Syndrome Critical region 8 (DGCR8) and an enzyme called Drosha ribonuclease (RNase III), convert these pri-mRNAs into pre-miRNA in the nucleus. pre-miRNA is then transported into cytoplasm and is cleaved by the RNase Dicer to create a miRNA-miRNA duplex. The double-strained miRNA is then separated into the functional strand and loaded together with Argonaute proteins into the RNA-induced silencing complex (RISC). This complex binds specific mRNAs, regulating degradation and translation of the mRNA targets. (Figure 12) Acting on the specific targets, miRNAs seem to have a fundamental role in the regulation of important cellular functions, such as proliferation, apoptosis, death, stress response, differentiation and development, and dysregulation of miRNA is associated with a variety of disorders. (48-51)

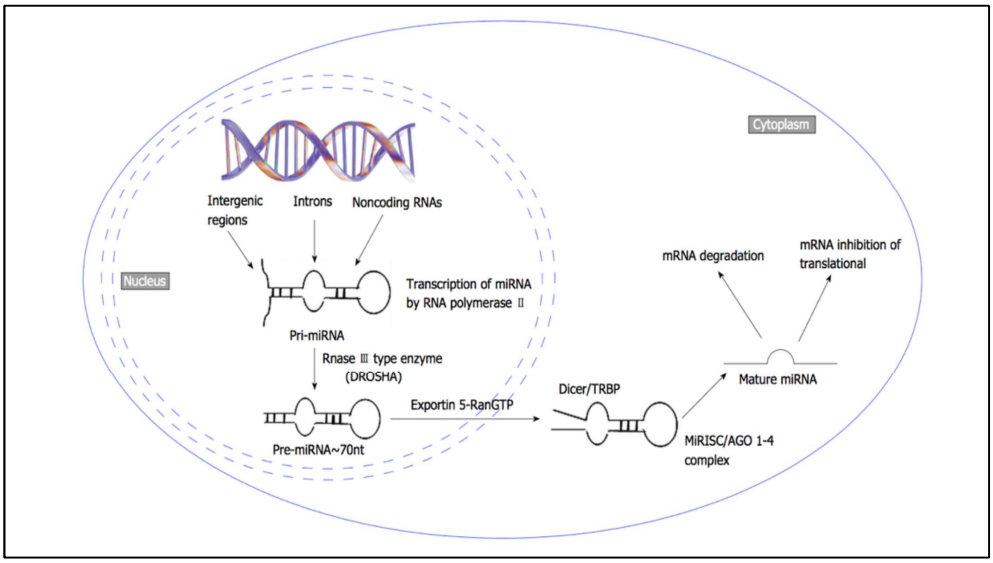

Figure 9- microRNA maturation and action (51)

1.4.2. MicroRNA and pregnancy

Placenta is the central organ for healthy pregnancy and studies regarding the placental miRNAs are important to understand the regulatory mechanisms of normal and complicated pregnancies. (52,53)

Placental miRNAs include placenta-specific, placenta-associated, and placenta-derived circulating miRNAs. While placenta-specific miRNAs are expressed largely or uniquely in the placental tissue, placenta-associated miRNAs are expressed ubiquitously in the placenta and other tissues. Placenta-derived circulating miRNAs refer to the circulating miRNA released from placenta. (52)

The first observation of placenta-enriched miRNAs was in 2004. (54)

Many of the placenta-specific miRNAs are located as a cluster on their respective chromosomes and are regulated by the same promoter. C19MC, a cluster on chromosome 19, was first identified in 2009 (55), followed by C14MC, a cluster

on chromosome 14, and miR-371-3 cluster, also on chromosome 19. (56) Until now, studies of placenta-specific miRNAs in the regulation of pregnancy are very limited focusing only on the basic biological characteristics.

Placenta-specific miRNAs, including C19MC family, were differentially expressed in various development steps, in order to meet the different regulatory demands during pregnancy. (50)

Placenta-associated miRNAs are expressed ubiquitously in placenta and other tissues. Like placenta-specific miRNAs, the placenta-associated miRNAs show different expression profiles in the trophoblast cells, placental tissue, and maternal plasma at different gestational ages. (52)

The possible role of miRNAs in normal and complicated pregnancy were studied partly. For example, it was demonstrated that placenta-specific miRNAs, miR-141 and miR-519d-3p (a member of C19MC), regulate trophoblast cell proliferation, invasion, migration, and intercellular communication. Furthermore, many placental miRNAs members of the miR- 17~92 cluster, miR-106a~363 and miR-106b~25 were significantly downregulated to facilitate syncytiotrophoblast differentiation. (57) Knockdown of global miRNA synthesis and individual miRNA, such as miR-675, enhanced trophoblast proliferation. (58,59)

Reversely, some miRNAs were upregulated to enable trophoblast proliferation, migration, and invasion.

A recent study on miRNA profiles in human placenta identified 191 differentially expressed microRNAs between first and third-trimester placentas, including placenta-specific and placenta- associated microRNAs. (60)

This study showed that oncogenic, angiogenic, and anti-apoptotic miRNAs were mainly expressed in the first-trimester placentas, whereas expression of miRNAs related to cell differentiation and tumour suppression was predominant in the third-trimester placentas. Furthermore, in the maternal plasma, a substantial amount of placental-associated miRNAs was differently expressed during the first-, second-, and third-trimester gestation. (61)

Different expression of miRNAs in the placenta during gestation depends on regulatory demand of the physiological change, such as inflammation and hypoxia. (62)

There are many miRNAs that are associated with preeclampsia.

Recent studies show that miRNAs related to the dysregulation of trophoblast and stem cell function are also associated with pathophysiology of preeclampsia. Some miRNAs, which regulate trophoblast cell proliferation, invasion, migration, and angiogenesis, were dysregulated in preeclamptic placentas. (63-66) Furthermore, miRNAs that regulate important physiological signalling pathways are also implicated in preeclampsia.

Placenta-associated miRNAs can also be implicated in other pregnancy complications, such as small-for-gestational age (SGA), or IUGR, or in some maternal-related pregnancy disorders, for example, preterm birth and abortion. (52)

There are some studies about miRNAs in the maternal circulation to identify their expression profile and explore the diagnostic potential. The placental-specific C19MC members were first discovered in the maternal blood and proved to be released from the trophoblasts via exosomes. (67)

Upregulation of circulating C19MC miRNAs was discovered in preeclampsia onset. It is interesting that circulating miRNAs members of the placenta-specific clusters can be found in the maternal and foetal circulation, but not in the men or non-pregnant women blood. These data introduce the possibility of the use of miRNAs as potential biomarkers in pregnancy. Foetal DNA and RNA, including miRNA, are present in the maternal circulation and serve as important diagnostic tools for healthy pregnancy and foetal disease. (68)

Foetal miRNAs are released in the circulation via exocytosis by exosomes and can act as mediators of cell-cell communication.

At the moment, there are no reports on foeto-maternal interaction of miRNAs. However, the possible regulatory roles of maternal miRNAs in foetal development and maternal pregnancy-associated disorders have been proposed. (69)

1.4.3. miR-125b

miR125 family is one of the most important miRNA families and it is composed of three homologs hsa-miR-125a, hsa-miR-125b-1 and hsa-miR-125b-2. miR-125-b1 and miR-125-b2 are two miRNAs that originate from different chromosomal loci, 11q24.1 and 21q21 respectively. Their mature sequence is miR-125b (Figure 13) (https://www.ncbi.nlm.nih.gov/gene/406911). (70-73)

Figure 10- miR-125b mature structure (http://www.mirbase.org/cgi-bin/mirna_entry.pl?acc=MIMAT0000423)

miR-125b is part of the *let-7* family, in particular of the let-7a-cluster. (60,72) Two major functions of let-7 family miRNAs seem to be the promotion of cell differentiation and tumour suppression.

Recent study indicates that *let-7* family miRNAs, including miR-125b, increase their expression during the physiological pregnancy, from first to third trimester, suggesting a critical role in regulating cell differentiation or placenta maturation (60), while Hromadnikova et al. showed a downregulation of miR-125b on maternal whole peripheral blood in PE compared to normal control. (66)

Previous studies showed that Trop2 mRNA is a target for the microRNA miR-125b. Nakanishi et al. first showed the correlation between miR-125b and Trop-2 in head and neck cancer. (74) Our recent study confirms the association between miR-125b and Trop-2 in bladder cancer. (39)

In both type of cancer, miR-125b decreases respect to normal tissue while Trop-2 expression increases, and the overexpression of miR-125b inhibits cell invasions and it corresponds to the decrease of Trop-2 protein level. (39,74)

2. Aim of the study

The aim of this study is to investigate the expression of Trop-2 and miR-125b during the physiological pregnancy and in preeclampsia, with or without IUGR, in order to verify if Trop-2 could be a target for miR-125b in placenta and to evaluate the possible role of miR-125b in the modulation of Trop-2 protein expression in normal or pathological human placenta tissues.

3. Materials and methods

3.1. Samples collection

In order to evaluate where Trop-2 is present in the physiological and pathological placentas, 40 human placentas were collected by the Department of Obstetrics and Gynecology, University of Turin (Italy), the Gynecology and Obstetrics Unit, Department of Clinical Sciences, Università Politecnica delle Marche (Ancona, Italy) and the Department of Obstetrics and Gynecology, Catholic University of Sacred Heart (Rome, Italy).

Normal placental tissues were obtained from voluntary terminations of pregnancy at 9-12 weeks of gestation (n=10) and from third trimester gestation delivery at 34-41 weeks (n=10) (Table 1).

Pathological placental tissues were collected after delivery from pregnant women affected by PE: 10 of them without IUGR (28-36 weeks of gestation) and 10 of them with IUGR (29-34 weeks of gestation) (Table 1).

Written informed consent was obtained from each pregnant woman and the permission of the Local Ethical Committee was granted for the study.

Samples for paraffin embedding were cut and immediately fixed in 4% neutral buffered formalin for 24 hours at 4 °C. The specimens were then processed with different grades of alcohol and xylene. Then, they were paraffin embedded at temperatures not exceeding 56 °C as previously described. (75)

Formalin fixed paraffin-embedded (FFPE) tissue sections of 2 µm, 3 µm and 10 µm were cut for immunofluorescence reactions, immunohistochemistry reactions and RNA extraction respectively.

Samples for protein extraction were cut and frozen at -80 °C until the use.

Plasma specimens were collected by Department of Obstetrics and Gynecology, University Hospital of Perugia, Perugia, Italy. Blood samples (n=22) were taken in tube with EDTA as anticoagulant from women at 12th weeks of gestation that had pregnancy without diseases (n=11) or with diagnosed PE (n=11) or PE-IUGR (n=3) after blood taking. Plasma samples were obtained centrifuging blood samples at 1500 g for 15 minutes at 4 °C and stored at -80 °C before use.

Table 1- Characteristic of physiological and pathological groups

	1st trimester (n=10)	3rd trimester (n=10)	PE (n=10)	PE-IUGR (n=10)
Maternal age (years)	30.2 ± 7.59	32.6 ± 4.05	36.9 ± 5.25	31.6 ± 3.81
Gestational age (weeks)	8.43 ± 1.95	37.25 ± 3.48	32.71 ± 3.85	30.81 ± 3.95

Table 1- Characteristics of physiological and pathological group of placenta tissue samples. Differences in maternal age are not significant (p=0.07); differences between gestational age are significant (p=0.0001)

3.2. Immunohistochemistry

Paraffin sections were deparaffinised and rehydrated via xylene and a graded series of ethyl alcohol. To inhibit endogenous peroxidase activity, sections were incubated with 3% hydrogen peroxide in methanol for 30' and treated with 0.3% Tween 20 in Phosphate Buffer Saline (PBS) 1X for 20' at room temperature for

antigen retrieval. Specimens were then washed in PBS 1X. To block nonspecific background, the sections were incubated with normal horse serum (Vector laboratories, California, USA) diluted 1:75 in PBS for 30'. Sections were incubated with mouse monoclonal antibody anti-Trop-2 (Table 2) overnight. After washing in PBS, the sections were subsequently incubated with horse anti-mouse biotinylated antibody diluted 1:200 (Vector Laboratories) for 30'. The peroxidase ABC method (Vector Laboratories) was performed and 3',3'-diaminobenzidine hydrochloride (Sigma-Aldrich, St Louis, MO, USA) as chromogenic was used. Sections were counterstained in Mayer's haematoxylin, dehydrated and mounted with Eukitt solution (Kindler GmbH and Co., Freiburg, Germany).

Negative control was performed omitting primary antibody. As positive control was used normal skin. (26)

Table 2- Primary antibodies used					
Antibody	**Specificity**	**Catalog**	**Application**	**Concentration**	**Source**
Mouse mAb	Human Trop-2	sc-376746	IHC, IF, WB	1:50 (IHC, IF) 1:250 (WB)	Santa Cruz Biotechnology, Santa Cruz, CA, USA)
Mouse mAb	Human BCL-2	M0887	IF	1:50	Dako, Glostrup, Denmark
Rabbit pAb	Human RKIP	07-137	IF	1:400	Upstate biotechnology, Lake Placid, NY, USA
Goat pAb	Human β-actin	sc-1616	WB	1:200	Santa Cruz Biotechnology, Santa Cruz, CA, USA)
Rabbit pAb	Human GAPDH	A300-641A-T	WB	1:1000	Bethyl Laboratories, Montgomery, TX, USA

Table 2- Primary antibodies used in immunohistochemistry, immunofluorescence and western blotting analyses. mAb: monoclonal antibody; pAb: polyclonal antibody; IHC: immunohistochemistry; IF: immunofluorescence; WB: western blotting.

3.3. Immunofluorescence

Samples were deparaffinised and hydrated with xylene and graded alcohol scale. To reduce autofluorescence, samples were incubated with 0,1% Sudan Black B

(Sigma-Aldrich) in 70° ethanol for 30' and then washed four times with PBS 1X with 0,03% Tween 20. For antigen retrieval, the slides were incubated with Tris-EDTA buffer pH 9 at 95 °C for 30' in Trop-2-BCL-2 double staining reaction and with 0.3% Tween 20 in PBS for 20' at room temperature in Trop-2-RKIP double staining reaction, and then washed twice with PBS 1X.

Non-specific sites were blocked in 3% BSA in PBS 1X for 30' and then the sections were incubated with mouse monoclonal anti-Trop-2 antibody (Table 2) overnight at 4 °C. Tissues were washed three times in order to remove unbound primary antibody with PBS, incubated with anti-mouse secondary antibodies Alexa Fluor 594 (1:400 dilution, Invitrogen, Life Technologies, Carlsbad, CA, USA) for 30'. After washing, specimens were incubated with mouse monoclonal BCL-2 (Table 2) or with RKIP (Table 2), both overnight at 4 °C. Samples were washed three times and incubated with donkey anti-mouse (for BCL-2) or donkey anti-rabbit (for RKIP) Alexa Fluor® 488 secondary antibodies (1:400 dilution, Invitrogen) for 30'. After incubation, slides were washed, incubated with TO-PRO-3® Iodide (1:3000 dilution, Invitrogen) for 10' for nuclear staining, then washed in PBS and mounted onto a glass slide using Vectashield mounting medium (Vector Labs). Sections were analysed by a motorized Leica DM6000 microscope at different magnifications. Fluorescence was detected with a Leica TCS-SL spectral confocal microscope equipped with an Argon and He/Ne mixed gas laser. Fluorophores were excited with the 488, 543, and 649nm lines and imaged separately. Images (1024 × 1024 pixels) were obtained sequentially from two channels using a confocal pinhole of 1.1200 and stored as TIFF files.

3.4. Cell culture

HTR-8 SVneo is a cell line obtained from immortalized extravillous trophoblast cells at first trimester of gestation. (76) The cells were cultured in RPMI-1640 medium (Euroclone S.p.A., Pero, Milan, Italy) with 10% FBS (Gibco, Life Technologies), 1% penicillin, 1% streptomycin, 1% L-glutamine at 37 °C, 21% O_2 and 5 % CO_2.

BeWo is a cell line obtained from immortalized choriocarcinoma cells. (77) The cells were cultured in Dulbecco's Modified Eagle Medium (DMEM) (Euroclone S.p.A.) and Ham's F12 (Euroclone S.p.A.) in ratio 1:1 supplemented with 10% FBS, 1% penicillin, 1% streptomycin at 37 °C, 21% O_2 and 5% CO_2. In order to stimulate syncytialization, BeWo cells were seeded in 6-well plates ($2{,}5x10^5$ cells for each well) and after overnight incubation after seeding, the medium was removed and replaced with fresh medium containing 20 μM forskolin (Sigma-Aldrich) or 0,2% DMSO as control and cells were incubated for another 48 hours as previously described. (78)

In order to mimic hypoxic condition as in preeclampsia, BeWo cells are incubated at 37 °C, 3% O_2, 92% N_2, 5% CO_2.

3.5. Cell transfection

$2{,}5x10^5$ cells were seeded in 6-well plates and transfected with the transfection complex, constituted by X-tremeGene 9 DNA Transfection Reagent (Roche Applied Science, Penzberg, Germany) and mirVana miRNA mimic (#MC10148 MIMAT0000423, Ambion, Life Technologies) or mirVana miRNA inhibitor (#MH10148 MIMAT0000423, Ambion, Life Technologies). The ratio between

transfecting agent and mimic or inhibitor was 6:1 and the final oligonucleotide concentration was 30 nM. Cells were incubated for 48 hours.

3.6. Western blotting

For protein extraction, tissue specimens were homogenized by Ultra-Turrax T8 (IKA-WERKE, Lille, France) in Lysis buffer containing 0.1 % SDS, 1 % NONIDET-P40, 1 mM orthovanadate sodium, 12 mM deoxycholate sodium, 1 mM PMSF, 1.7 µg/ml aprotinin in PBS buffer 1x and then centrifuged at 16000 g for 20 minutes at 4 °C. Pellets were discarded and supernatants were collected and stored at -80 °C until use.

For protein extraction from cells, pellets were collected and incubated in ice with Lysis buffer for 30 minutes and then centrifuged at 14000 g for 20 minutes at 4 °C. Supernatants were aliquoted and stored at -80 °C before the use.

To determine protein concentration, the Bradford protein assay with Bio-Rad Protein Assay Dye Reagent Concentrate was performed (Bio-Rad Laboratories, Milan, Italy). Different concentrations of BSA in distilled water were used to draw the standard curve. All protein samples (50 µg of protein for each sample) were fractionated in 15% SDS-PAGE gel and electrophoretically transferred to Trans-Blot Turbo Mini Nitrocellulose membranes (Bio-Rad Laboratories) with Trans-Blot Turbo Transfer System (Bio-Rad Laboratories).

Membranes were incubated with 5% milk in distilled water to block nonspecific sites for 1h 30' and then with monoclonal mouse antibody anti-Trop-2 (Table 2) in TBS with 0,05% Tween 20 (TBS-T) at 4 °C overnight. After washing with TBS-T, membranes were incubated with secondary antibody anti-mouse

conjugated with horseradish peroxidase (Santa Cruz Biotechnology) at 1:1500 dilution. Detection of antibody binding was performed with the Clarity Western ECL Substrate (Bio-Rad Laboratories) and images were acquired with Chemidoc (Bio-Rad Laboratories). Densitometric analysis was performed with ImageJ Software (https://imagej.nih.gov/ij/download.html). GAPDH and β-actin were used as housekeeping to normalize cell and tissue values respectively (Table 2).

Western blotting on Trop-2 expression on transfected BeWo cells permitted to confirm that miR-125b downregulates Trop-2 expression.

3.7. RNA extraction, retrotranscription and real time PCR

3.7.1. FFPE tissue samples

Total RNA for miRNA analysis was extracted from formalin-fixed paraffin-embedded tissue samples by FFPE RNA/DNA Purification Kit (Norgen Biotek Corp., Thorold, Canada) as written in manufacturer's protocol.

The sections were deparaffinized in xylene at 60 °C for 5 minutes and then centrifuged at 14000 g for 2 minutes. The supernatants were removed and the pellets were washed by ethanol. After centrifugation at 14000 rpm for 2 minutes, the supernatants were removed and pellets air-dried.

The pellets were digested with the Proteinase K at 55 °C for 15 minutes and then at 80 °C for 15 minutes. Binding solution and ethanol were added to lysates, and then loaded into a spin-column and centrifuged at 14000 g for 1 minute. Under these conditions only the RNAs were bound to column while most of the contaminants were removed. Columns were then washed in order to remove any

impurities and centrifuged for 1 minute. Total RNAs were eluted in 40 µl of elution buffer and stored at -80 C until use.

3.7.2. Cell samples

For RNA extraction, cells seeded in 6-well plates were lysed with TRIzol reagent (Ambion, Life Technologies, Carlsbad, CA, USA); lysates were collected and RNA purified with Direct-zol RNA MiniPrep kit (Zymo Research Corp., Irvine, CA, USA) according to the manufacturer's recommendations. Same amount of ethanol absolute and TRIzol with lysate cell were mixed and then loaded into a spin-column and centrifuged at 14000 g for 1 minute.

Subsequently, the spin-column was loaded with RNA pre-wash and centrifuged and washed with buffer. To elute the RNA bind, the column was loaded with DNase/RNase-free water and centrifuge.

Total RNAs were stored at -80 °C until use.

3.7.3. Retrotranscription and Real Time PCR

Retrotranscription (RT) was performed using TaqMan microRNA Reverse Transcription kit (Applied Biosystem, Life Technologies) and specific primer TaqMan microRNA Assays for miR-125b and RNU48 (a constituent nucleolar RNA that was used for normalization) (Table 1). For each retrotranscription reaction, were used 3.34 µl of RNA sample for a total volume of 10 µl. For the reaction of RT, the thermocycler worked on the following temperature and time: 16 °C for 30 min, 42 °C for 30 min and 85 °C for 5 min. Temperature was then lead to 4 °C.

For real time PCR, Taqman Fast Universal PCR Master Mix (Applied Biosystem, Life Technologies) and probes for miR-125b and RNU48 (Table 1) were used. cDNA was 4.5 µl in 10 µl of total volume. All PCR reactions were performed in duplicates and the negative controls as water instead of cDNA sample did not generate any signal during PCR reactions. The thermocycler executed 40 cycles of the following program for the real time PCR reactions: 95 °C for 10 min, 95 °C for 15 seconds and 60 °C for 1 min. The threshold cycle value (C_t) was defined as the fractional cycle number at which signal passes a fixed threshold. The relative amount of each target miRNA to RNU48 was calculated using the equation $2^{-\Delta Ct}$, where $\Delta C_t = C_{t\ miR\text{-}125b} - C_{t\ RNU48}$.

Table 3- Primers and probes for retrotranscription and real time PCR			
miRNA/snoRNA	**Catalog**	**Assay ID**	**Source**
miR-125b	#4427975	#000449	Applied Biosystem, Life Technologies
RNU 48	#4427975	#001006	Applied Biosystem, Life Technologies

Table 3- Primers and probes for retrotranscription and real time PCR analyses

Real time PCR on transfected cells permitted to confirm that transfection occurred.

3.8. Statistical analysis

Due to the small sample size and the non-normal distribution, the expression of Trop-2 and miR-125b in physiological and pathological specimens was tested with non-parametric approaches. MiR-125b levels were analysed after log transformation. Median and interquartile range (IQR) were used as a measure of centrality and variability, respectively, and graphically represented as boxplots. Trop-2 levels were analysed as the mean ± standard deviation (SD) and represented as histograms.

The Mann-Whitney test was applied to between two group comparisons, while the Kruskal-Wallis test was applied to between three group comparisons.

Graphpad Prism 7 program was used for the analyses and a probability of 0.05 was set as the threshold for statistical significance.

4. Results

4.1. Trop-2 expression and quantification

In order to determine where Trop-2 is expressed in the placenta and how the expression changes during the physiological pregnancy, immunohistochemical analysis was performed in first and third trimester placenta specimens from physiological pregnancy and in placenta specimens affected by PE, with or without IntraUterine Growth Restriction.

Normal human skin was used as positive control. Trop-2 was localized in the epidermis, but the cells of the basal layer were negative. A progressive staining was detected in all the other layers, showing a stronger expression in the cells of the corneum layer (Figure 11) as previously described. (26)

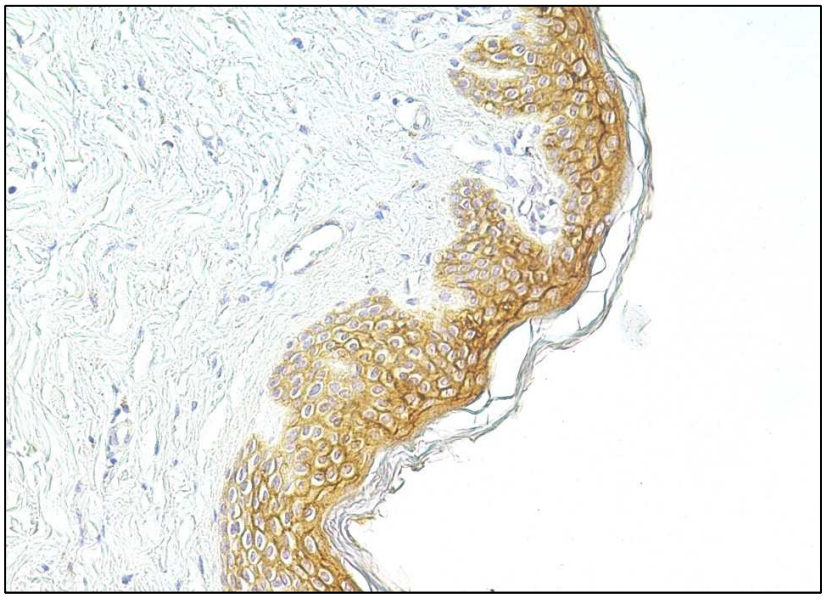

Figure 11- Trop-2 immunostaining in human skin used as positive control (40X magnification)

Immunofluorescence was performed to detail more about Trop-2 localization in placenta tissue. Semiquantitative assays were conducted by western blotting, in

order to evaluate Trop-2 level during normal and pathological pregnancy and in vitro analyses.

4.1.1. First and third trimester of gestation

Immunostaining on placenta samples showed the location of Trop-2 in trophoblast, between syncytiotrophoblast and cytotrophoblast (Figure 12, 13, 14). In first trimester samples, Trop-2 expression was weak (Figure 12A, 12B, 14A), while third trimester samples showed a strong Trop-2 expression (Figure 12C, 12D, 14B). These data suggest an increase of Trop-2 protein during the normal development of the placenta and the normal course of pregnancy.

Cell islands adjacent to villi in first trimester placenta were not stained while the staining is present in the villous trophoblast (Figure 13).

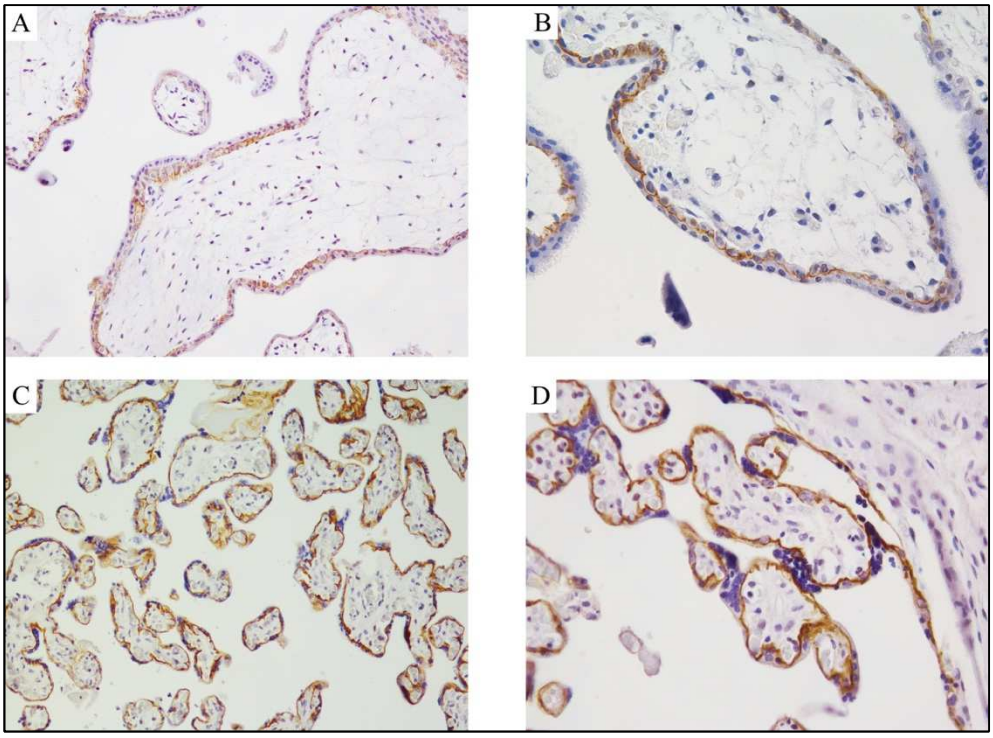

Figure 12- Immunohistochemical staining of Trop-2 protein in physiological placenta tissues. A, B: first trimester placenta; C, D: third trimster placenta. (A, C: 20X magnification; B, D: 40X magnification)

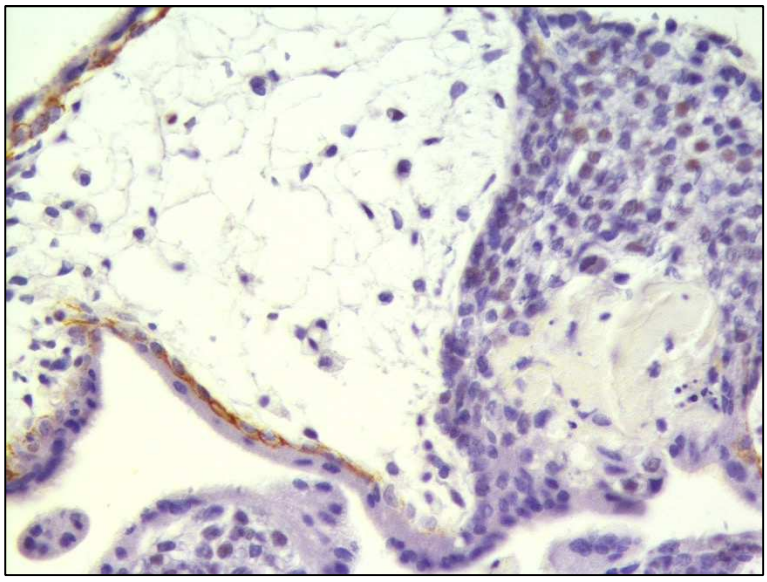

Figure 13- First trimester villus and cell island (40X magnification)

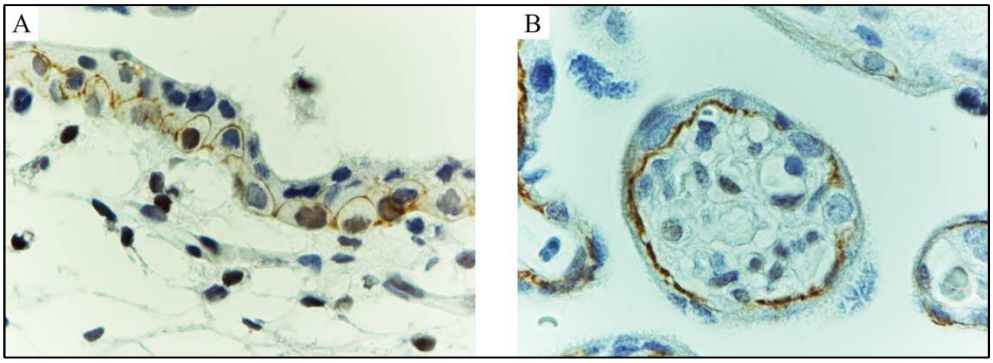

Figure 14- Particular of trophoblast of a first trimester villus (A); third trimester villus (B) (A, B: 100X magnification with immersion oil)

Immunofluorescence analysis was performed to detail more about Trop-2 position in the trophoblast. RKIP was used as marker of cytotrophoblast in first trimester placenta while BCL-2 was used as marker of syncytiotrophoblast in first and third trimester placenta as previously demonstrated. (79,80)

Double-labelling reaction with Trop-2 (Figure 15A) and RKIP (Figure 15B) didn't show co-localization (Figure 15D).

Double-labelling reactions with Trop-2 (Figure 16A, 17A) and BCL-2 (Figure 16B, 17B) in first (Figure 16) and third (Figure 17) trimester placenta showed sites of co-localization, represented by yellow colour, demonstrating that Trop-2 is located in the basal membrane of syncytiotrophoblast.

Furthermore, extravillous trophoblast HTR8/SVneo cell line did not show Trop-2 expression in western blotting analysis (Figure 18A), while BeWo cell line with induced syncytialization showed Trop-2 expression (Figure 18B). All these data demostrate that Trop-2 protein is localised in syncytiotrophoblast, in particular in the basal membrane.

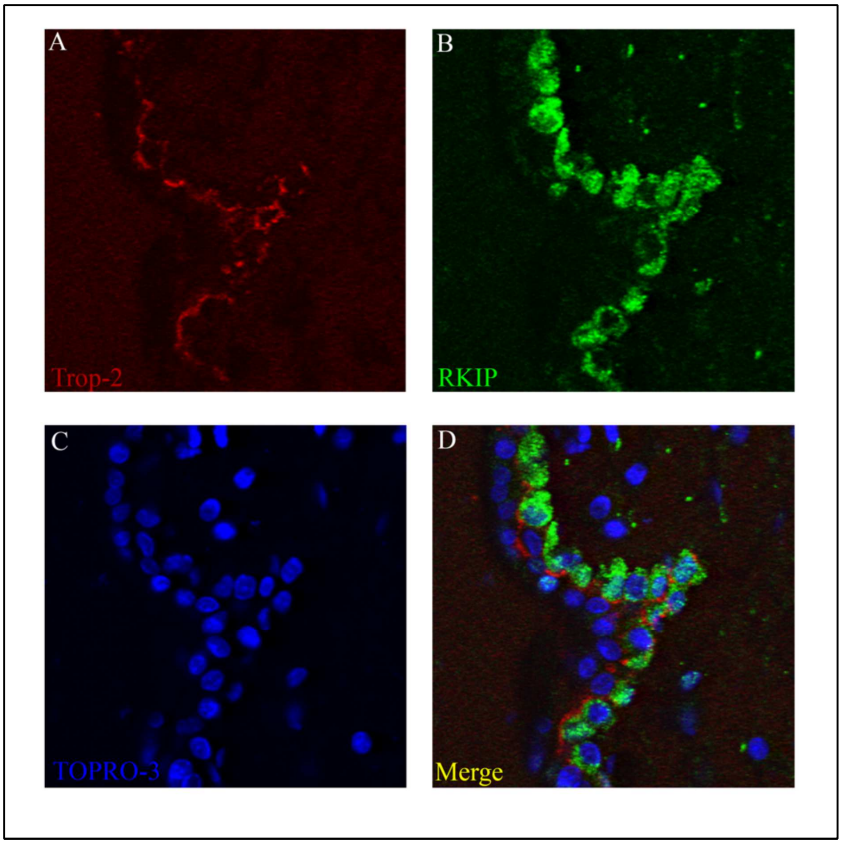

Figure 15- Double-labelling immunofluorescence staining in first trimester placenta. Trop-2 staining (A); RKIP staining (B); Nuclear staining (C); Merge (D) (60X magnification)

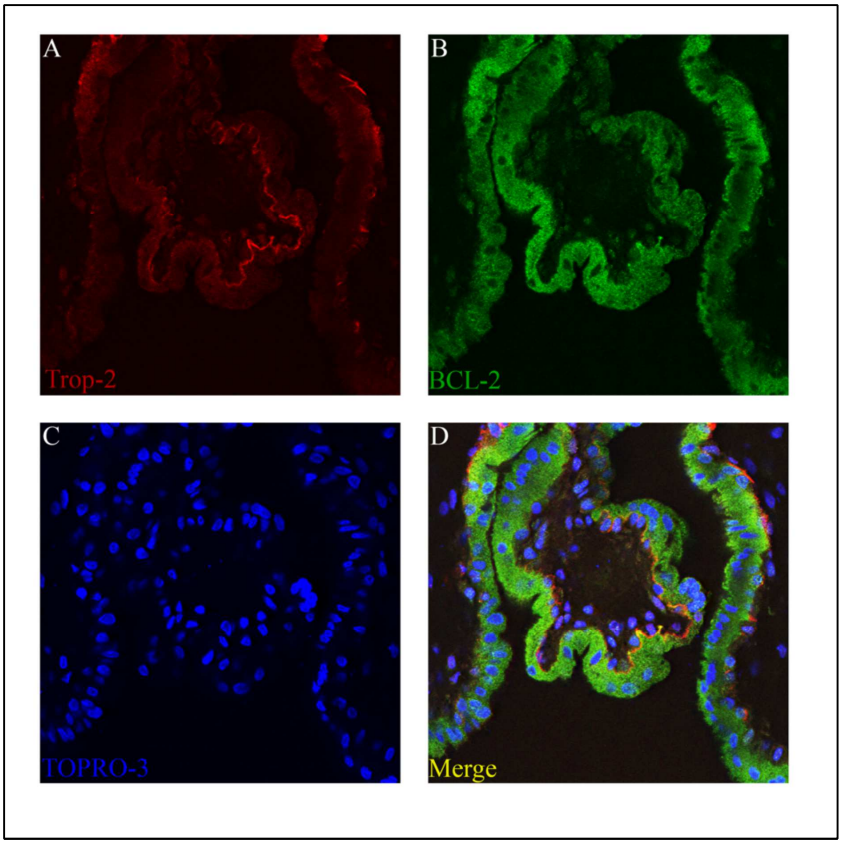

Figure 16- Double-labelling immunofluorescence staining in first trimester placenta. Trop-2 staining (A); BCL-2 staining (B); Nuclear staining (C); Merge (D) (40X magnification)

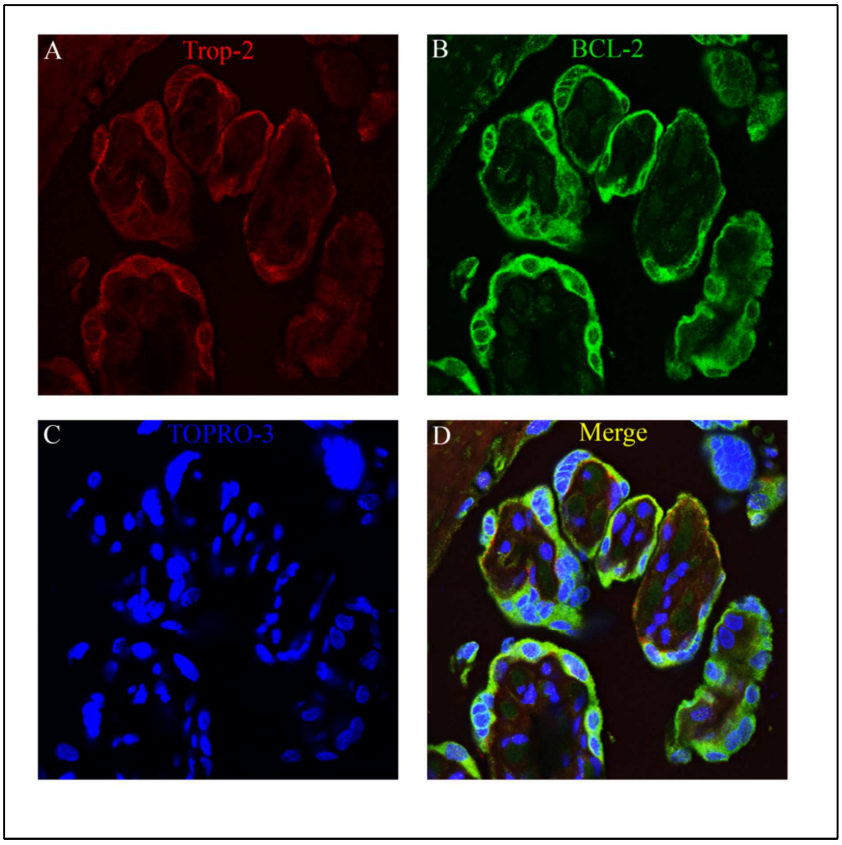

Figure 17- Double-labelling immunofluorescence staining in third trimester placenta. Trop-2 staining (A); BCL-2 staining (B); Nuclear staining (C); Merge (D) (40X magnification)

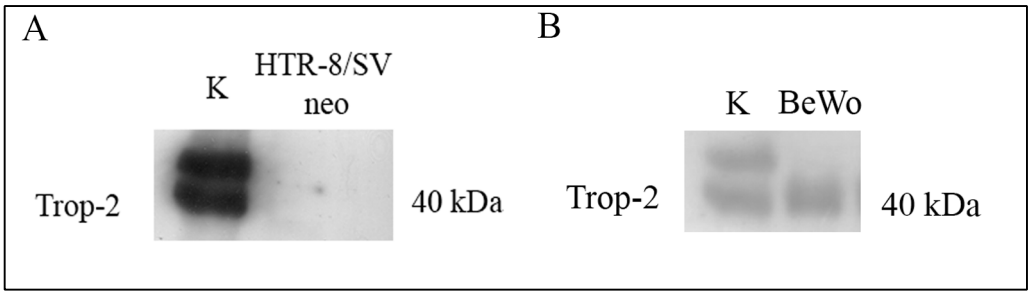

Figure 18- Representative western blotting of HTR8/SVneo (A) and BeWo with syncytialization inducted (B) cell line.

Figure 19 shows the semiquantitative summarized analysis on Trop-2 expression.

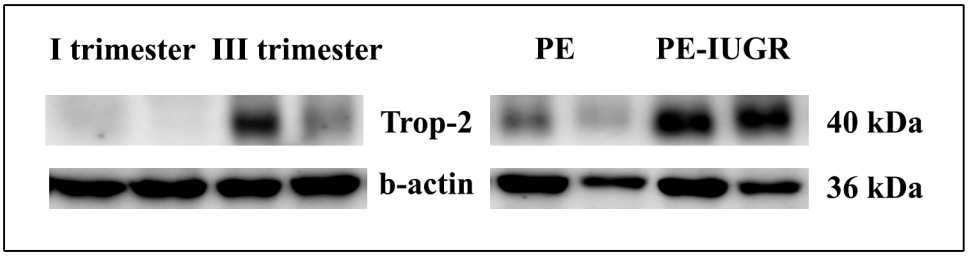

Figure 19- Representative western blotting of physiological (first and third trimester) and pathological (PE and PE-IUGR) samples.

A progressive increase of Trop-2 level was found in physiological pregnancy (Figure 19, 20). First trimester tissues showed a modest Trop-2 expression, while the protein increased its expression in third trimester (p=0.01), demonstrating the increasing level of Trop-2 during the placenta development.

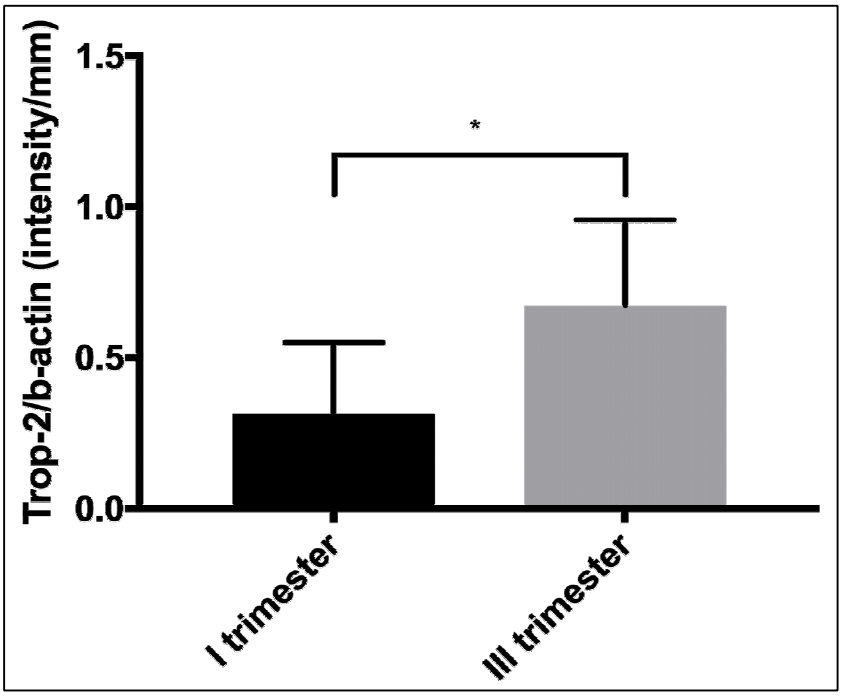

Figure 20- Representative histogram of western blotting analysis of physiological specimens. Trop-2 expression increases during the physiological pregnancy (: p=0.01)*

4.1.2. Preeclampsia and preeclampsia complicated by Intrauterine Growth Restriction

Immunohistochemical analysis on placenta specimens from women affected by preeclampsia presented very weak Trop-2 expression (Figure 21A, 21B), while the staining was very strong in PE-IUGR placenta samples (Figure 21C, 21D).

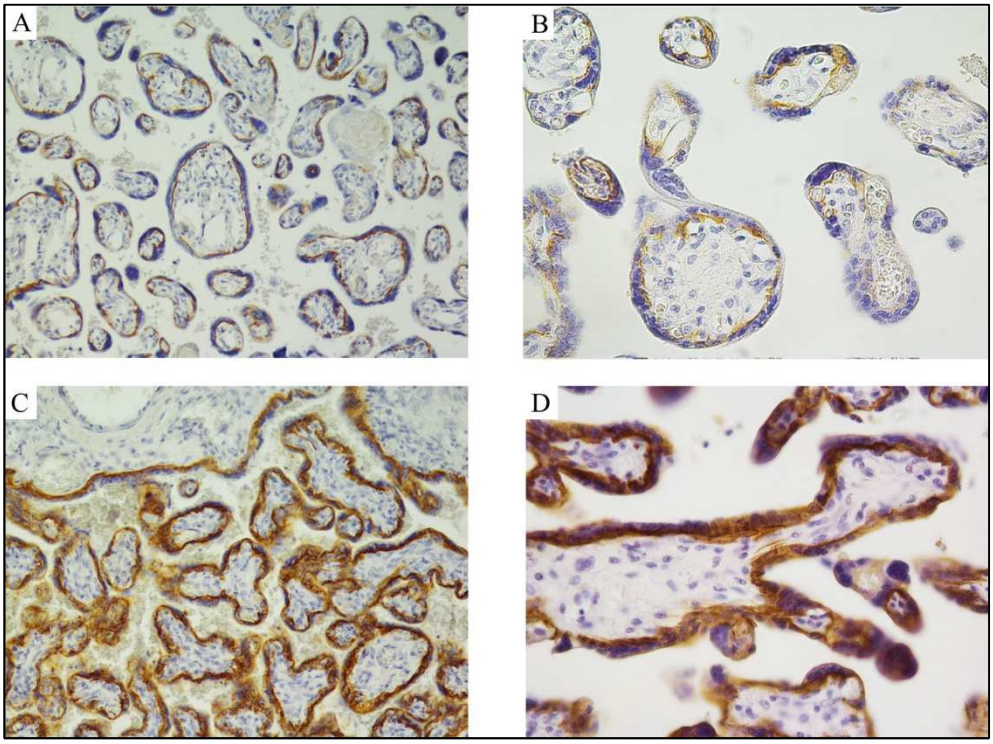

Figure 21- Trop-2 immunohistochemistry in pathological placenta tissues. A, B: Preeclampsia affected placenta; C, D: Preeclampsia affected placenta complicated by IntraUterine Growth Restriction. (A, C: 20X magnification; B, D: 40X magnification)

Trop-2 quantification in pathological pregnancy was evaluated by western blotting analysis (Figure 19, 22) showing that placenta tissues from pregnant with preeclampsia expressed very low level of Trop-2 compared to PE-IUGR specimens that, on the contrary, expressed a very strong Trop-2 staining ($p=0.0003$).

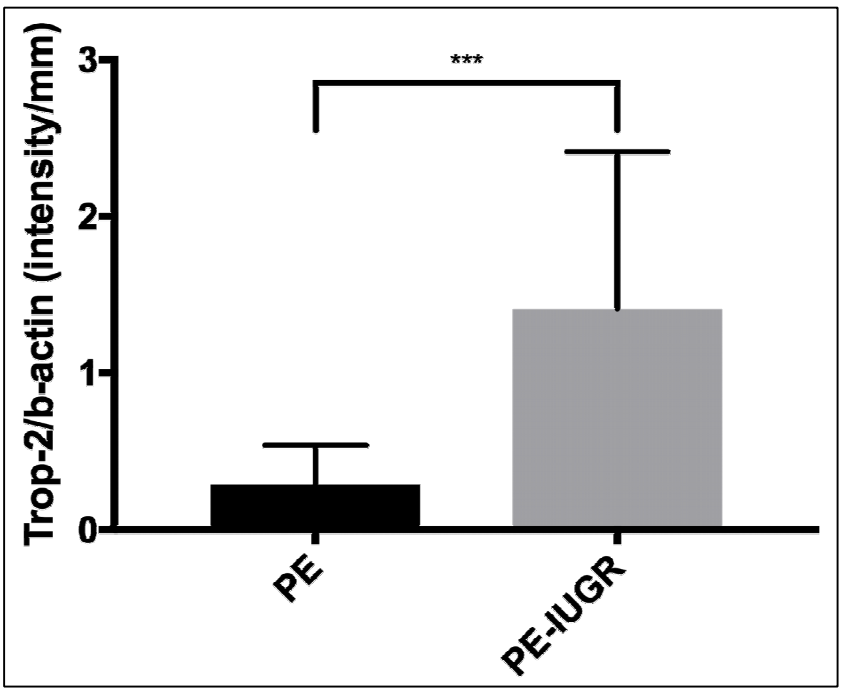

*Figure 22- Representative histogram of western blotting analysis. In PE specimens Trop-2 expression in lower than in PE-IUGR specimens (***: p=0.0003).*

In vitro analyses confirmed in vivo data. BeWo cells treated with forskolin (to induce syncytialization) and cultured in hypoxic conditions (to mimic preeclamptic conditions) showed lower Trop-2 level than those cultured at normal atmospheric conditions (p=0.03) (Figure 23).

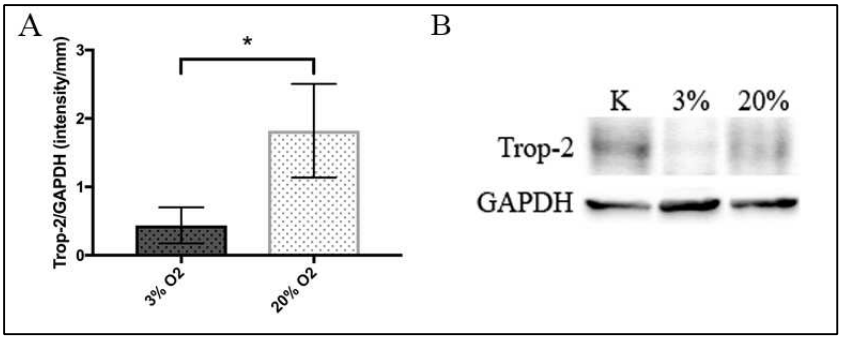

Figure 23- Representative western blot of BeWo at syncytium induced at 3% and 20% O_2 condition. Representative histogram shows the lower Trop-2 expression in cells cultured at 3% O_2 compared to 20% O_2 (A) (: p=0.03); representative image of western blotting (B).*

4.1.3. Conclusions

Trop-2 expression increased during the normal gestation (Figure 19, 20). In PE placenta, Trop-2 expression was very weak, while was very high in PE-IUGR (Figure 19, 22). A trend line with physiological values obtained by western blotting analysis was drawn in order to extrapolate a possible Trop-2 expression value at 32.71 and 30.81 weeks of gestation. Presumed values can be used to compare PE and PE-IUGR samples with control of corresponding gestational age. Observed Trop-2 value in PE samples was lower than the presumed value at the same gestational age in physiological conditions (Figure 24), while Trop-2 level in PE-IUGR was higher than in presumed value at the same gestational age (Figure 24). In vitro analyses confirmed that Trop-2 level decreases in hypoxic condition (Figure 23), that is typical condition of PE pathology.

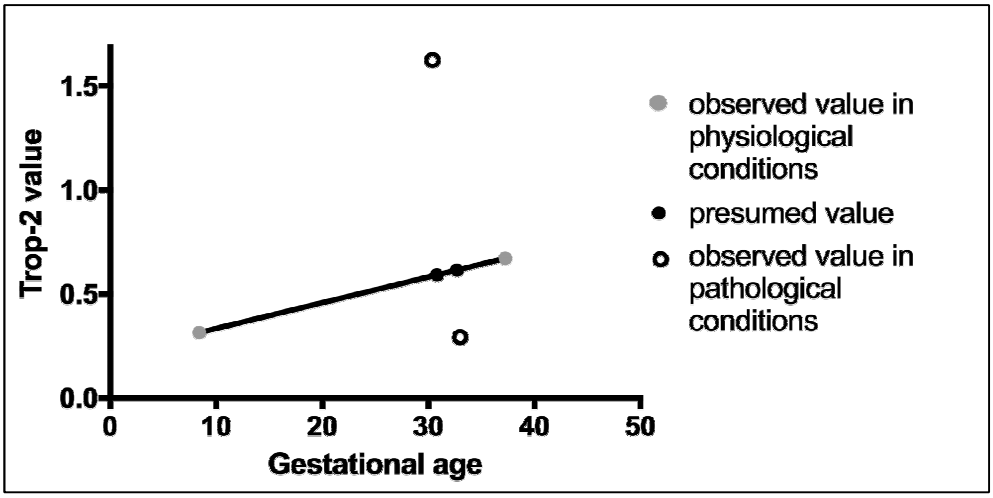

Figure 24- Representative tend line for Trop-2 expression. Observed value in PE condition is lower than presumed PE value and observed value in PE-IUGR condition is 2.5-fold higher than presumed PE-IUGR value according to tend line. The values are expressed as mean.

4.2. miR-125b expression

To explore the possible role of miR-125b on Trop-2 expression, miR-125b levels were analysed by real time PCR on FFPE placenta tissue (first and third trimester, PE and PE-IUGR) and plasma collected at first trimester of pregnancy.

4.2.1. First and third trimester

On FFPE tissues, miR-125b level increased during the physiological pregnancy (Figure 25). In fact, miR-125b was low expressed in first trimester tissue, while in third trimester tissue the expression was higher (**: p=0.002).

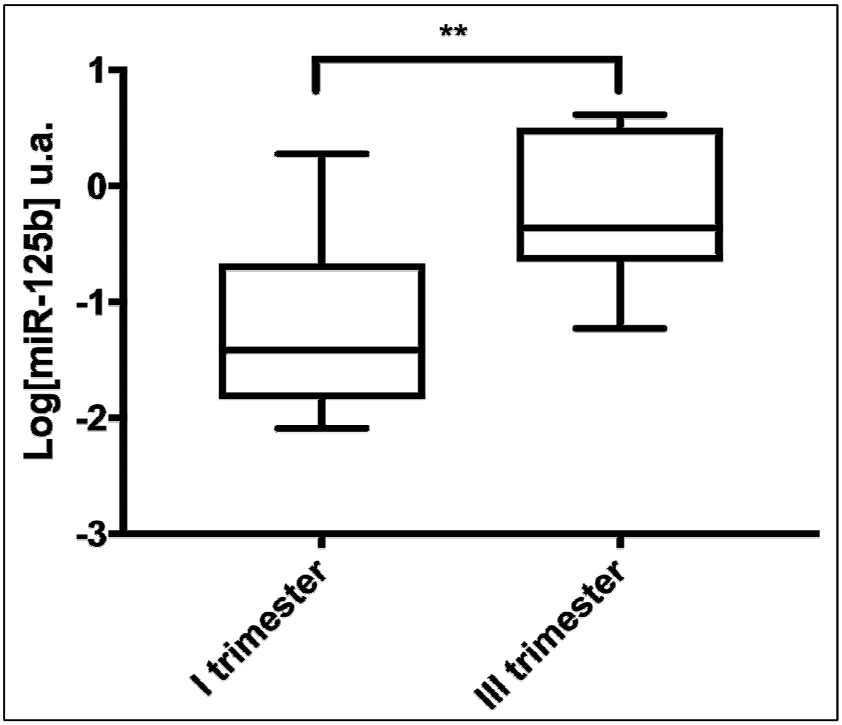

*Figure 25- Representative box plot of Real Time PCR in first and third trimester placenta. miR-125b level increases during physiological pregnancy (**:p=0.002)*

4.2.2. Preeclampsia and preeclampsia complicated by Intrauterine Growth Restriction

Real time PCR on FFPE pathological tissues showed no significant differences and PE and PE-IUGR specimens (Figure 26).

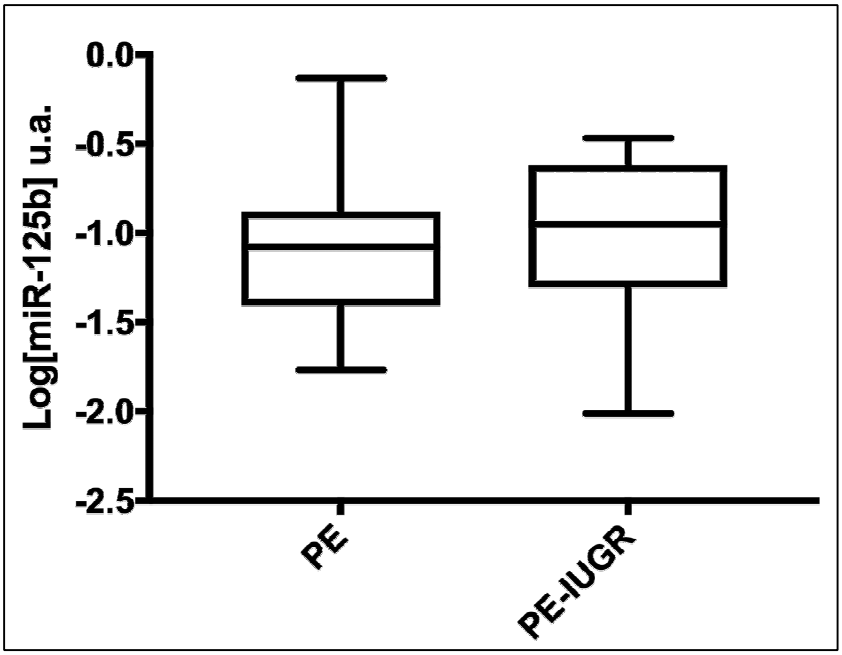

Figure 26- Representative box plot of real time PCR of FFPE placenta tissue affected by PE and PE-IUGR. No significant differences are present between specimens with and without IUGR (p=0.496).

4.2.3. Conclusions

miR-125b expression increased during the normal gestation (Figure 25). In PE and PE-IUGR samples, miR-125b didn't show differences in expression (Figure 26). A trend line with physiological values obtained by western blotting analysis was drawn in order to extrapolate a possible miR-125b expression value at 32.71 and 30.81 weeks of gestation. Presumed values can be used to compare PE and PE-IUGR samples with control of corresponding gestational age. Observed miR-125b value in PE and in PE-IUGR samples was lower than the presumed value at the same gestational age in physiological conditions (Figure 27). These data seem to indicate an equilibrium between miR-125b and Trop-2 during the physiological pregnancy and a dysfunctional relation between the two molecules in PE disease.

Figure 27- Representative tend line for miR-125b expression. Observed values in PE and PE-IUGR conditions are lower than presumed PE and PE-IUGR values according to tend line. The values are expressed as median.

4.3. miR-125b in first trimester plasma

In first trimester maternal plasma, miR-125b was higher in women who developed PE than in controls (p=0.01), suggesting that maternal circulating miR-125b could influence Trop-2 expression during the first phase of placental development in pregnant women that will develop PE but not in PE-IUGR (Figure 28).

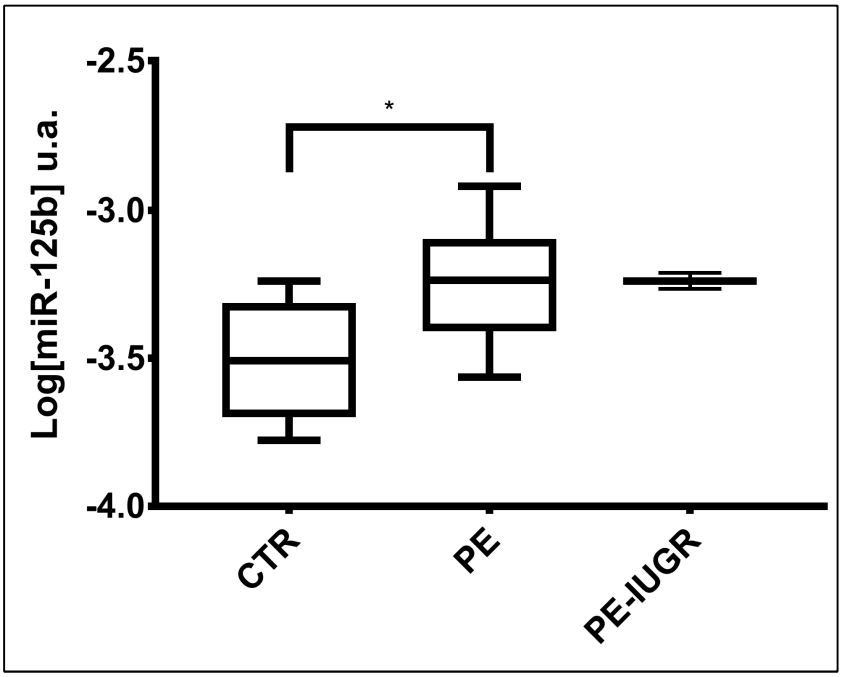

Figure 28-Representative box plot of real time PCR of 1st trimester plasma. Trop-2 level in PE is higher compared to normal control (: p=0.01). Differences are not significant between control and PE-IUGR (p=0.08) and PE and PE-IUGR (p=0.09).*

5. Discussion

Trop-2 was first identified by Lipinski in 1981 as a marker for trophoblast cells and choriocarcinoma cell lines. (23) These authors did not identify the cellular type expressing Trop-2 as well as they did not study the role of this protein in placental tissues, but they showed generally the localization of this protein in the trophoblast. No other study is present in literature about Trop-2 expression in placenta. Our research showed the specific Trop-2 location in placenta and the expression in normal and pathological pregnancy. Morphological and in vitro analyses demonstrated that Trop-2 is located in the basal part of syncytiotrophoblast, suggesting that Trop-2 can have a role in maintenance of morphology and function of syncytiotrophoblast during the placental development.

Trop-2 level increased during the physiological pregnancy, endorsing the theory of its role in syncytiotrophoblast development and maintenance.

This placental behaviour changes in pathological conditions, i.e. Trop-2 is weakly expressed in PE and increased in PE-IUGR placenta tissue. These two pathologies are characterised by an altered development of syncytiotrophoblast showing many apoptotic figures due to hypoxic conditions, especially in PE pathology. (3)

These results can suggest that Trop-2 placed in the basal membrane of syncytiotrophoblast has a role in maintenance of syncytiotrophoblast integrity, acting on the cell-cell adhesion. The increase of Trop-2 expression in third trimester of pregnancy could be related to the decreased fusion of cytotrophoblastic cells with the overlying syncytiotrophoblast. At the end of pregnancy, the placenta is definitely grown and the new formation of

syncytiotrophoblast is an infrequent event. Its low expression in PE tissue suggests that Trop-2 could influence the cytotrophoblast fusion, so the syncytiotrophoblast is badly developed and consequently the placenta doesn't work properly.

These data are supported by the role of Trop-2 in cell-cell adhesion as previously demonstrate in other tissue models (22, 27).

miR-125b is a microRNA of *let-7a* cluster miRNAs that have two major functions: promotion of cell differentiation and tumour suppression. Gu et al. (60) showed that the expression of tumour suppressor miRNAs (including miR-125b) increases in term placenta. Probably, these miRNAs participate in placenta maturation and play a role in limiting placental tissue growth when pregnancy toward term. Our data confirm the increase of miR-125b expression at third trimester respect to first trimester placenta, showing a balance between Trop-2 and miR-125b. In both PE and PE-IUGR, placental miR-125b is low expressed, suggesting that the balance is broken. In PE-IUGR tissues, the high level of Trop-2 and the low level of miR-125b suggest that placental miR-125b fails its control on Trop-2 expression.

On the contrary, in PE placenta tissues Trop-2 and miR-125b are both downregulated, suggesting other mechanisms to control Trop-2 expression.

Our data on plasma collected at first trimester of pregnancy showed higher levels of miR-125b in women who developed PE subsequently compared to control. These data suggest that maternal circulating miR-125b could control Trop-2 expression at the early stages of pregnancy in women that will be affect by preeclampsia.

These results propose that in PE Trop-2 expression could be under maternal control through circulating miR-125b, while in PE-IUGR there is not the maternal regulation and placental miR-125b can't regulate Trop-2 expression.

These data support previous papers that consider PE and PE-IUGR as two different pathologies with two different etiopathogenesis. (81-84)

Our analyses showed two different behaviour and two different control of the Trop-2/miR-125b axis, supporting this thesis.

In fact, while in normal pregnancy Trop-2 and miR-125b seem to collaborate to the correct development of placenta, in PE and PE-IUGR they do not maintain this mechanism. In PE, Trop-2 seems to be under control of maternal circulating miR-125b that prevents the protein expression. In PE-IUGR, maternal circulating and placental miR-125b cannot control the Trop-2 expression levels and the protein is overexpressed.

Our work on maternal plasma at 12 weeks of gestation is a preliminary study that paves the way to future studies that can be focused on the role of Trop-2 protein and miR-125b in physiological and pathological conditions in order to investigate a possible use of both as early biomarkers of PE and PE-IUGR using maternal plasma.

6. References

1. Myatt L. Role of placenta in preeclampsia. Endocrine. 2002 Oct 1;19(1):103–11.

2. Ma O, Mateer J, Reardon R, Joing S. Ma and Mateer's Emergency Ultrasound. Third edition. McGraw-Hill; 2014.

3. Benirschke K, Kaufmann P, Baergen RN. Pathology of the human placenta. Fitfth edition. Springer; 2006.

4. ACOG Committee on Obstetric Practice. Practice bulletin #33: diagnosis and management of preeclampsia and eclampsia. Obstet Gynecol. 2002 Jan 1;99(1):159–67.

5. Steegers EA, von Dadelszen P, Duvekot JJ, Pijnenborg R. Pre-eclampsia. The Lancet. 2010 Aug 27;376(9741):631–44.

6. Goulopoulou S, Davidge ST. Molecular mechanisms of maternal vascular dysfunction in preeclampsia. Trends Mol Med. 2015 Feb;21(2):88–97.

7. Perucci LO, Corrêa MD, Dusse LM, Gomes KB, Sousa LP. Resolution of inflammation pathways in preeclampsia—a narrative review. Immunol Res. 2017 Aug 1;65(4):774–89.

8. Herzog EM, Eggink AJ, Reijnierse A, Kerkhof MAM, de Krijger RR, Roks AJM, et al. Impact of early- and late-onset preeclampsia on features of placental and newborn vascular health. Placenta. 2017 Jan;49:72–9.

9. Crispi F, Llurba E, Domínguez C, Martín-Gallán P, Cabero L, Gratacós E.

Predictive value of angiogenic factors and uterine artery Doppler for early- versus late-onset pre-eclampsia and intrauterine growth restriction. Ultrasound Obstet Gynecol. 2008 Mar 1;31(3):303–9.

10. Berzan E, Doyle R, Brown CM. Treatment of Preeclampsia: Current Approach and Future Perspectives. Curr Hypertens Rep. 2014 Sep 1;16(9):473.

11. Sibai B, Dekker G, Kupferminc M. Pre-eclampsia. The Lancet. 2005 Mar 4;365(9461):785–99.

12. Soleymanlou N, Jurisicova A, Wu Y, Chijiiwa M, Ray JE, Detmar J, et al. Hypoxic switch in mitochondrial myeloid cell leukemia factor-1/Mtd apoptotic rheostat contributes to human trophoblast cell death in preeclampsia. Am J Pathol. 2007 Aug;171(2):496–506.

13. Armant DR, Fritz R, Kilburn BA, Kim YM, Nien JK, Maihle NJ, et al. Reduced expression of the epidermal growth factor signaling system in preeclampsia. Placenta. 2015 Mar;36(3):270–8.

14. Lorenzi T, Marzioni D, Giannubilo S, Quaranta A, Crescimanno C, De Luca A, et al. Expression Patterns of Two Serine Protease HtrA1 Forms in Human Placentas Complicated by Preeclampsia with and without Intrauterine Growth Restriction. Placenta. 2009 Jan;30(1):35–40.

15. Heazell AEP, Moll SJ, Jones CJP, Baker PN, Crocker IP. Formation of syncytial knots is increased by hyperoxia, hypoxia and reactive oxygen species. Placenta. 2007 Apr;28 Suppl A:S33-40.

16. Zhang S, Regnault TRH, Barker PL, Botting KJ, McMillen IC, McMillan

CM, et al. Placental adaptations in growth restriction. Nutrients. 2015 Jan 8;7(1):360–89.

17. Smith SC, Baker PN, Symonds EM. Increased placental apoptosis in intrauterine growth restriction. Am J Obstet Gynecol. 1997 Dec;177(6):1395–401.

18. Scifres CM, Nelson DM. Intrauterine growth restriction, human placental development and trophoblast cell death. J Physiol. 2009 Jul 15;587(Pt 14):3453–8.

19. Redline RW. Placental Pathology: A Systematic Approach with Clinical Correlations. Placenta. 2008 Mar 1;29:86–91.

20. Marzioni D, Lorenzi T, Altobelli E, Giannubilo SR, Paolinelli F, Tersigni C, et al. Alterations of maternal plasma HTRA1 level in preeclampsia complicated by IUGR. Placenta. 2012 Dec;33(12):1036–8.

21. Cross JC. Placental function in development and disease. Reprod Fertil Dev. 2006;18(1–2):71–6.

22. McDougall ARA, Tolcos M, Hooper SB, Cole TJ, Wallace MJ. Trop2: From development to disease. Dev Dyn. 2015 Feb 1;244(2):99–109.

23. Lipinski M, Parks DR, Rouse RV, Herzenberg LA. Human trophoblast cell-surface antigens defined by monoclonal antibodies. Proc Natl Acad Sci U S A. 1981 Aug;78(8):5147–50.

24. Pavšič M, Ilc G, Vidmar T, Plavec J, Lenarčič B. The cytosolic tail of the tumor marker protein Trop2 - a structural switch triggered by phosphorylation. Sci

Rep [Internet]. 2015 May 18 [cited 2017 Aug 30];5. Available from: http://www.ncbi.nlm.nih.gov/pmc/articles/PMC4434849/

25. Guerra E, Trerotola M, Aloisi AL, Tripaldi R, Vacca G, La Sorda R, et al. The Trop-2 signalling network in cancer growth. Oncogene. 2013 Mar 21;32(12):1594–600.

26. Stepan LP, Trueblood ES, Hale K, Babcook J, Borges L, Sutherland CL. Expression of Trop2 Cell Surface Glycoprotein in Normal and Tumor Tissues. J Histochem Cytochem. 2011 Jul;59(7):701–10.

27. Nakatsukasa M, Kawasaki S, Yamasaki K, Fukuoka H, Matsuda A, Tsujikawa M, et al. Tumor-Associated Calcium Signal Transducer 2 Is Required for the Proper Subcellular Localization of Claudin 1 and 7. Am J Pathol. 2010 Sep;177(3):1344–55.

28. McDougall ARA, Hooper SB, Zahra VA, Sozo F, Lo CY, Cole TJ, et al. The oncogene Trop2 regulates fetal lung cell proliferation. Am J Physiol - Lung Cell Mol Physiol. 2011 Oct 1;301(4):L478–89.

29. Liu T, Liu Y, Bao X, Tian J, Liu Y, Yang X. Overexpression of TROP2 Predicts Poor Prognosis of Patients with Cervical Cancer and Promotes the Proliferation and Invasion of Cervical Cancer Cells by Regulating ERK Signaling Pathway. PLOS ONE. 2013 set;8(9):e75864.

30. Cubas R, Zhang S, Li M, Chen C, Yao Q. Trop2 expression contributes to tumor pathogenesis by activating the ERK MAPK pathway. Mol Cancer. 2010 Sep 21;9:253.

31. Ripani E, Sacchetti A, Corda D, Alberti S. Human Trop-2 is a tumor-associated calcium signal transducer. Int J Cancer. 1998 May 29;76(5):671–6.

32. Stoyanova T, Goldstein AS, Cai H, Drake JM, Huang J, Witte ON. Regulated proteolysis of Trop2 drives epithelial hyperplasia and stem cell self-renewal via β-catenin signaling. Genes Dev. 2012 Oct 15;26(20):2271–85.

33. Lin J-C, Wu Y-Y, Wu J-Y, Lin T-C, Wu C-T, Chang Y-L, et al. TROP2 is epigenetically inactivated and modulates IGF-1R signalling in lung adenocarcinoma. EMBO Mol Med. 2012 Jun;4(6):472–85.

34. Fong D, Spizzo G, Gostner JM, Gastl G, Moser P, Krammel C, et al. TROP2: a novel prognostic marker in squamous cell carcinoma of the oral cavity. Mod Pathol Off J U S Can Acad Pathol Inc. 2008 Feb;21(2):186–91.

35. Ning S, Liang N, Liu B, Chen X, Pang Q, Xin T. TROP2 expression and its correlation with tumor proliferation and angiogenesis in human gliomas. Neurol Sci Off J Ital Neurol Soc Ital Soc Clin Neurophysiol. 2013 Oct;34(10):1745–50.

36. Bignotti E, Todeschini P, Calza S, Falchetti M, Ravanini M, Tassi RA, et al. Trop-2 overexpression as an independent marker for poor overall survival in ovarian carcinoma patients. Eur J Cancer. 2010 Mar 1;46(5):944–53.

37. Ohmachi T, Tanaka F, Mimori K, Inoue H, Yanaga K, Mori M. Clinical Significance of TROP2 Expression in Colorectal Cancer. Clin Cancer Res. 2006 May 15;12(10):3057–63.

38. Mühlmann G, Spizzo G, Gostner J, Zitt M, Maier H, Moser P, et al.

TROP2 expression as prognostic marker for gastric carcinoma. J Clin Pathol. 2009 Feb;62(2):152–8.

39. Avellini C, Licini C, Lazzarini R, Gesuita R, Guerra E, Tossetta G, et al. The trophoblast cell surface antigen 2 and miR-125b axis in urothelial bladder cancer. Oncotarget. 2017 Aug 29;8(35):58642–53.

40. Wang J, Day R, Dong Y, Weintraub SJ, Michel L. Identification of Trop-2 as an oncogene and an attractive therapeutic target in colon cancers. Mol Cancer Ther. 2008 Feb 1;7(2):280–5.

41. Trerotola M, Cantanelli P, Guerra E, Tripaldi R, Aloisi AL, Bonasera V, et al. Upregulation of Trop-2 quantitatively stimulates human cancer growth. Oncogene. 2013 Jan 10;32(2):222–33.

42. Trerotola M, Jernigan DL, Liu Q, Siddiqui J, Fatatis A, Languino LR. Trop-2 promotes prostate cancer metastasis by modulating β1 integrin functions. Cancer Res. 2013 May 15;73(10):3155–67.

43. Fong D, Moser P, Krammel C, Gostner JM, Margreiter R, Mitterer M, et al. High expression of TROP2 correlates with poor prognosis in pancreatic cancer. Br J Cancer. 2008 Oct 21;99(8):1290–5.

44. Wu H, Xu H, Zhang S, Wang X, Zhu H, Zhang H, et al. Potential therapeutic target and independent prognostic marker of TROP2 in laryngeal squamous cell carcinoma. Head Neck. 2013 Oct;35(10):1373–8.

45. Chen R, Lu M, Wang J, Zhang D, Lin H, Zhu H, et al. Increased expression of Trop2 correlates with poor survival in extranodal NK/T cell

lymphoma, nasal type. Virchows Arch. 2013 Nov 1;463(5):713–9.

46. Lin H, Zhang H, Wang J, Lu M, Zheng F, Wang C, et al. A novel human Fab antibody for Trop2 inhibits breast cancer growth in vitro and in vivo. Int J Cancer. 2014 Mar 1;134(5):1239–49.

47. Lee RC, Feinbaum RL, Ambros V. The C. elegans heterochronic gene lin-4 encodes small RNAs with antisense complementarity to lin-14. Cell. 1993 Dec 3;75(5):843–54.

48. Paul P, Chakraborty A, Sarkar D, Langthasa M, Rahman M, Bari M, et al. Interplay between miRNAs and human diseases. J Cell Physiol. 2017 Feb 9;

49. Shiiba M, Shinozuka K, Saito K, Fushimi K, Kasamatsu A, Ogawara K, et al. MicroRNA-125b regulates proliferation and radioresistance of oral squamous cell carcinoma. Br J Cancer. 2013 May 14;108(9):1817–21.

50. Morales-Prieto DM, Chaiwangyen W, Ospina-Prieto S, Schneider U, Herrmann J, Gruhn B, et al. MicroRNA expression profiles of trophoblastic cells. Placenta. 2012 Sep 1;33(9):725–34.

51. Shah NR, Chen H. MicroRNAs in pathogenesis of breast cancer: Implications in diagnosis and treatment. World J Clin Oncol. 2014 May 10;5(2):48–60.

52. Cai M, Kolluru GK, Ahmed A. Small Molecule, Big Prospects: MicroRNA in Pregnancy and Its Complications. J Pregnancy [Internet]. 2017 [cited 2017 Sep 7];2017. Available from: http://www.ncbi.nlm.nih.gov/pmc/articles/PMC5496128/

53. Mouillet J-F, Chu T, Sadovsky Y. Expression patterns of placental microRNAs. Birt Defects Res A Clin Mol Teratol. 2011 Aug;91(8):737–43.

54. Barad O, Meiri E, Avniel A, Aharonov R, Barzilai A, Bentwich I, et al. MicroRNA expression detected by oligonucleotide microarrays: System establishment and expression profiling in human tissues. Genome Res. 2004 Dec;14(12):2486–94.

55. Luo S-S, Ishibashi O, Ishikawa G, Ishikawa T, Katayama A, Mishima T, et al. Human Villous Trophoblasts Express and Secrete Placenta-Specific MicroRNAs into Maternal Circulation via Exosomes. Biol Reprod. 2009 Oct 1;81(4):717–29.

56. Morales-Prieto DM, Ospina-Prieto S, Chaiwangyen W, Schoenleben M, Markert UR. Pregnancy-associated miRNA-clusters. J Reprod Immunol. 2013 Mar 1;97(1):51–61.

57. Kumar P, Luo Y, Tudela C, Alexander JM, Mendelson CR. The c-Myc-Regulated MicroRNA-17~92 (miR-17~92) and miR-106a~363 Clusters Target hCYP19A1 and hGCM1 To Inhibit Human Trophoblast Differentiation. Mol Cell Biol. 2013 May;33(9):1782–96.

58. Forbes K, Farrokhnia F, Aplin JD, Westwood M. Dicer-dependent miRNAs provide an endogenous restraint on cytotrophoblast proliferation. Placenta. 2012 Jul 1;33(7):581–5.

59. Gao W, Liu M, Yang Y, Yang H, Liao Q, Bai Y, et al. The imprinted H19 gene regulates human placental trophoblast cell proliferation via encoding miR-

675 that targets Nodal Modulator 1 (NOMO1). RNA Biol. 2012 Jul 1;9(7):1002–10.

60. Gu Y, Sun J, Groome LJ, Wang Y. Differential miRNA expression profiles between the first and third trimester human placentas. Am J Physiol - Endocrinol Metab. 2013 Apr 15;304(8):E836–43.

61. Li H, Guo L, Wu Q, Lu J, Ge Q, Lu Z. A comprehensive survey of maternal plasma miRNAs expression profiles using high-throughput sequencing. Clin Chim Acta. 2012 Mar 22;413(5):568–76.

62. Challis JR, Lockwood CJ, Myatt L, Norman JE, Strauss JF, Petraglia F. Inflammation and Pregnancy. Reprod Sci. 2009 Feb 1;16(2):206–15.

63. Li P, Guo W, Du L, Zhao J, Wang Y, Liu L, et al. microRNA-29b contributes to pre-eclampsia through its effects on apoptosis, invasion and angiogenesis of trophoblast cells. Clin Sci. 2013 Jan 1;124(1):27–40.

64. Bai Y, Yang W, Yang H, Liao Q, Ye G, Fu G, et al. Downregulated miR-195 Detected in Preeclamptic Placenta Affects Trophoblast Cell Invasion via Modulating ActRIIA Expression. PLoS ONE [Internet]. 2012 Jun 19 [cited 2017 Sep 14];7(6). Available from: http://www.ncbi.nlm.nih.gov/pmc/articles/PMC3378540/

65. Luo L, Ye G, Nadeem L, Fu G, Yang BB, Honarparvar E, et al. MicroRNA-378a-5p promotes trophoblast cell survival, migration and invasion by targeting Nodal. J Cell Sci. 2012 Jul 1;125(13):3124–32.

66. Hromadnikova I, Kotlabova K, Hympanova L, Krofta L. Gestational

hypertension, preeclampsia and intrauterine growth restriction induce dysregulation of cardiovascular and cerebrovascular disease associated microRNAs in maternal whole peripheral blood. Thromb Res. 2016 Jan 1;137(Supplement C):126–40.

67. Donker RB, Mouillet JF, Chu T, Hubel CA, Stolz DB, Morelli AE, et al. The expression profile of C19MC microRNAs in primary human trophoblast cells and exosomes. Mol Hum Reprod. 2012 Aug;18(8):417–24.

68. Go ATJI, Vugt V, M.g J, Oudejans CBM. Non-invasive aneuploidy detection using free fetal DNA and RNA in maternal plasma: recent progress and future possibilities. Hum Reprod Update. 2011 May 1;17(3):372–82.

69. Bullerdiek J, Flor I. Exosome-delivered microRNAs of "chromosome 19 microRNA cluster" as immunomodulators in pregnancy and tumorigenesis. Mol Cytogenet. 2012 Jul 2;5:27.

70. Yin H, Sun Y, Wang X, Park J, Zhang Y, Li M, et al. Progress on the relationship between miR-125 family and tumorigenesis. Exp Cell Res. 2015 Dec 10;339(2):252–60.

71. Sun Y-M, Lin K-Y, Chen Y-Q. Diverse functions of miR-125 family in different cell contexts. J Hematol OncolJ Hematol Oncol. 2013 Jan 15;6:6.

72. Wong KY, Yu L, Chim CS. DNA methylation of tumor suppressor miRNA genes: a lesson from the miR-34 family. Epigenomics. 2011 Feb;3(1):83–92.

73. Kim K-H, Bin B-H, Kim J, Dong SE, Park PJ, Choi H, et al. Novel

inhibitory function of miR-125b in melanogenesis. Pigment Cell Melanoma Res. 2014 Jan;27(1):140–4.

74. Nakanishi H, Taccioli C, Palatini J, Fernandez-Cymering C, Cui R, Kim T, et al. Loss of miR-125b-1 contributes to head and neck cancer development by dysregulating TACSTD2 and MAPK pathway. Oncogene. 2014 Feb 6;33(6):702–12.

75. Mühlhauser J, Crescimanno C, Kaufmann P, Höfler H, Zaccheo D, Castellucci M. Differentiation and proliferation patterns in human trophoblast revealed by c-erbB-2 oncogene product and EGF-R. J Histochem Cytochem. 1993 Feb 1;41(2):165–73.

76. Graham CH, Hawley TS, Hawley RG, MacDougall JR, Kerbel RS, Khoo N, et al. Establishment and characterization of first trimester human trophoblast cells with extended lifespan. Exp Cell Res. 1993 Jun;206(2):204–11.

77. Prakash GJ, Suman P, Gupta SK. Relevance of Syndecan-1 in the Trophoblastic BeWo Cell Syncytialization. Am J Reprod Immunol. 2011 Nov 1;66(5):385–93.

78. Orendi K, Gauster M, Moser G, Meiri H, Huppertz B. The choriocarcinoma cell line BeWo: syncytial fusion and expression of syncytium-specific proteins. Reproduction. 2010 Nov 1;140(5):759–66.

79. Ciarmela P, Marzioni D, Islam MS, Gray PC, Terracciano L, Lorenzi T, et al. Possible role of RKIP in cytotrophoblast migration: immunohistochemical and in vitro studies. J Cell Physiol. 2012 May 1;227(5):1821–8.

80. Marzioni D, Mühlhauser J, Crescimanno C, Banita M, Pierleoni C, Castellucci M. BCL-2 expression in the human placenta and its correlation with fibrin deposits. Hum Reprod Oxf Engl. 1998 Jun;13(6):1717–22.

81. Grisaru-Granovsky S, Halevy T, Eidelman A, Elstein D, Samueloff A. Hypertensive disorders of pregnancy and the small for gestational age neonate: not a simple relationship. Am J Obstet Gynecol. 2007 Apr;196(4):335.e1-5.

82. Soto E, Romero R, Richani K, Espinoza J, Chaiworapongsa T, Nien JK, et al. Preeclampsia and pregnancies with small-for-gestational age neonates have different profiles of complement split products. J Matern Fetal Neonatal Med. 2010 Jul;23(7):646–57.

83. Huppertz B. Trophoblast differentiation, fetal growth restriction and preeclampsia. Pregnancy Hypertens. 2011 Jan;1(1):79–86.

84. Huppertz B, Weiss G, Moser G. Trophoblast invasion and oxygenation of the placenta: measurements versus presumptions. J Reprod Immunol. 2014 Mar;101–102:74–9.